STATE OF HEALTH DETERMINATION OF BATTERIES AT VARIOUS OPERATING CONDITIONS

by

Prashanth Ganeshram

A Thesis Presented in Partial Fulfillment
of the Requirements for the Degree
Master of Science in Technology

Approved April 2014 by the
Graduate Supervisory Committee:

Arunachalanadar Madakannan, Chair
Xihong Peng
Changho Nam

ARIZONA STATE UNIVERSITY

May 2014

ABSTRACT

Objective of the study is to get a clear idea on the cyclic performance of duty operation of Batteries. Batteries are an integral part of solar plants and wind energy farms due to the fact that energy storage is vital in these places. Various types of losses related to the performance are clearly analyzed and studied. Assessment of State Of Health and State Of Charge is critical in order to maximize the performance and lifetime of a battery. Batteries were subjected to temperature and charge/discharge rate variations and found that the state of health degradation was severe at high temperature along with faster rate of charging compared to other evaluation conditions. The entire research was conducted at the Alternative Energy Technology Laboratory located at Arizona State University, Mesa. It involved the use of various instruments namely the Programmable Voltage Regulator for charging, Computerized Battery Analyzer and Programmable Electric Load for discharging and also the PARSTAT potentiostat for measuring the impedance of various battery technologies under study. At first, the Batteries were discharged and based on the time taken, it was charged for the next cycle. Impedance measurement was done at regular cycle intervals in order to study the degradation of health. For every cycle, the battery capacity was also calculated and noted down. . The results obtained show that low and stable impedance over the given cycle life is an important consideration in the selection of batteries according to the applications

DEDICATION

I would like to dedicate this work to my parents USHA GANESHRAM and S.GANESHRAM, my family, relatives and friends back in India for their extended support. They deserve all the credits for what I am at present.

ACKNOWLEDGEMENT

To begin with, I would like to thank Dr. Arunachalanadar Madakannan for allowing me to work on the exact kind of project which I wanted to and also for his constant guidance and support. I would also like to thank Dr. Changho Nam and Dr. Xihong Peng for readily accepting to be my committee members. I would be very grateful to my colleague and friend Ximo Chu for constantly motivating and helping me out through the project. It's because of her that certain critical areas were brought to my knowledge and I was able to make myself better. My lab mates Sri Harsha Kolli and Stephen Annor-Wiafe deserve credit for the timely help they did by making themselves present when it was needed. Last but not least I would like to thank Surya V.J, Jayakrishna , Dilip , Rakhshanda, Hari, Venkatesh,Vidya, Swetha, Amrit, Anirudh, Ajay, Raghav, Sriram , Kashyap and Mani for sharing my burden over this two year period.

Table of Contents

CHAPTER Page

ABSTRACT i

DEDICATION ii

ACKNOWLEDGEMENT iii

LIST OF FIGURES vi

LIST OF TABLES ix

1. INTRODUCTION 1

1.1 Battery Technologies 1

1.2 Problem Statement 5

1.3 Scope and Purpose 5

2. LITERATURE REVIEW 7

2.1 Instruments used 7

2.2 Lithium ion Bulging 15

3. METHODOLOGY 20

3.1 Battery cycling 20

3.2 Impedance measurement 22

3.3 Regression Analysis 29

4. RESULTS 32

4.1 Mathematical Analysis 32

CHAPTER Page

4.2 Discharge curves 40

4.2 Impedance spectroscopy 47

4.3 HFR vs SOC 54

5. CONCLUSION 57

REFERENCES 59

LIST OF FIGURES

FIGURE	Page
1: NICKEL CADMIUM CELL	2
2: SEALED LEAD ACID CELLS	2
3: LITHIUM ION CELL	3
4: NICKEL METAL-HYDRIDE CELL	4
5: FLOWCHART FOR BATTERY CYCLING	6
6: COMPUTERIZED BATTERY ANALYZER	7
7: ELECTRONIC LOAD	8
8: POTENTIOSTAT	9
9: PROGRAMMABLE POWER SUPPLY FOR 8A CHARGING	10
10 : PROGRAMMABLE POWER SUPPLY FOR 2A CHARGING	10
11 : DAILY TIMER	12
12: WEEKLY TIMER	12
13: THERMAL CHAMBER FRONT VIEW	13
14: THERMAL CHAMBER SIDE VIEW	13
15: SPECIAL BASE FOR LI-ION CELLS INSIDE CHAMBER	14
16 : FLOW CHART FOR LI-ION BULGE RECOVERY	16
17 : BULGED CELL #3	16
18: BULGED CELL #3 (TOP VIEW)	17
19: BULGED CELL #2	17
20: BULGED CELL #4	18

FIGURE Page

21: SCREENSHOT OF CHARGING PROFILE 19

22: CHARGE AND DISCHARGE CURVE 20

23 : DAILY ROUTINE FOR BATTERY CYCLING (LI-ION) 21

24: IMPEDANCE SPECTROSCOPY OUTPUT GRAPHS OF CHARGED CELL AND DISCHARGED CELL RESPECTIVELY. 23

25: HIGH FREQUENCY RESISTANCE PLOT 24

26 : SCREENSHOT #1 OF POWERSUITE DIALOG BOX 25

27: SCREENSHOT #2 OF POWERSUITE DIALOG BOX 26

28: SCREENSHOT #3 OF POWERSUITE DIALOG BOX 27

29: SCREENSHOT OF IMPEDANCE SPECTROSCOPY OUTPUT GRAPHS OF A CHARGED LEAD ACID CELL 28

30: SAMPLE RESIDUAL PLOT #1 30

31 :SAMPLE RESIDUAL PLOT #2 31

32: SAMPLE RESIDUAL PLOT #3 31

33: SCREENSHOT OF MINITAB WORKSHEET #1 32

34: SCREENSHOT OF MINITAB WORKSHEET #2 33

35: SCREENSHOT OF MINITAB TOOLBAR 34

36: SCREENSHOT OF MINITAB DIALOG BOX #1 34

37: SCREENSHOT OF MINITAB DIALOG BOX #2 35

38: SCREENSHOT OF MINITAB RESULT #1 36

39: SCREENSHOT OF MINITAB RESULT #2 37

FIGURE Page

40 : RESIDUAL PLOT OF CAPACITY 38

41: RESIDUAL PLOT OF IMPEDANCE 39

42: DISCHARGE PROFILE OF LEAD ACID CELL #1 41

43: DISCHARGE PROFILE OF LEAD ACID CELL #2 42

44: DISCHARGE PROFILE OF LEAD ACID CELL #3 43

45: DISCHARGE PROFILE OF LEAD ACID CELL #4 44

46 : DISCHARGE PROFILE OF LI-ION CELL #2 45

47: DISCHARGE PROFILE OF LI-ION CELL #4 46

48: NYQUIST PLOT FOR LEAD ACID CELL #1 47

49: NYQUIST PLOT FOR LEAD ACID CELL #2 48

50: NYQUIST PLOT FOR LEAD ACID CELL #3 49

51: NYQUIST PLOT FOR LEAD ACID CELL #4 50

52: HIGH FREQUENCY RESISTANCE PLOTS FOR LEAD ACID CELLS 51

53: NYQUIST PLOT FOR LI-ION CELL #1 52

54: NYQUIST PLOT FOR LI-ION CELL #2 53

55: NYQUIST PLOT FOR LI-ION CELL #4 53

56: HIGH FREQUENCY RESISTANCE PLOT FOR LI-ION CELLS 54

57: HFR VS SOC TEST FOR LEAD ACID CELLS 55

LIST OF TABLES

TABLE Page

1: SEALED LEAD ACID BATTERY CONDITIONS 40

2 : HFR VS SOC DATA FOR LEAD ACID CELLS 56

CHAPTER ONE

1. INTRODUCTION

1.1 Battery Technologies

The scope of the research allows to test four different battery technologies namely Nickel Cadmium (Ni-Cd), Sealed Lead Acid (SLA), Lithium-ion (Li-ion) and Nickel Metal Hydride (Ni-MH). It is important to understand the battery chemistry and behavior before going on to determine which battery is best suited for which climatic or operating conditions.

Nickel Cadmium (Ni-Cd):

The maximum discharge rate for a Ni–Cd battery varies by size. For a common AA-size cell, the maximum discharge rate is approximately 1.8 amps whereas for a D size battery the discharge rate can be as 3.5 amps. The nominal cell potential is usually 1.2 V which is lower than the 1.5 V of alkaline and zinc–carbon primary cells. This is the reason why they are not appropriate as a replacement in all applications. Unlike alkaline and zinc–carbon primary cells, a Ni–Cd cell's terminal voltage only changes a little as it discharges. Because many electronic devices are designed to work with primary cells that may discharge to as low as 0.90 to 1.0 V per cell, the relatively steady 1.2 V of a Ni–Cd cell is enough to allow operation. [1, 2]



Figure 1: Nickel Cadmium Cell

Sealed Lead Acid (SLA):

In spite of the competition from Li-ion and NiMH batteries, the market for lead acid batteries grow, mainly in the large scale energy storage applications with wind or solar based renewable systems. In spite of their lowest energy density (< 50 Wh/kg), these batteries still enjoy the largest market share for major stationary energy storage applications due to the development of better grids with Ca and Ti additives and electrodes with Ga2O3 and Bi2O3 additives. Compared to the existing battery systems, these batteries fare extremely well in terms of availability, ease of use and maintainability, reliability, recycling as well the cost. [3]



Figure 2: Sealed Lead Acid Cells

Lithium-ion (Li-ion):

The voltage of a Li-poly cell varies from about 2.7 V (discharged) to about 4.23 V (fully charged), and Li-poly cells have to be protected from overcharge by limiting the applied voltage to no more than 4.235 V per cell used in a series combination. The nominal cell voltage being 3.7 V. There is a general notion that the cycle life of these cells can be up to a maximum of 1000 cycles. This type has technologically evolved from lithium-ion batteries. The primary difference is that the lithium-salt electrolyte is not held in an organic solvent but in a solid polymer composite such as polyethylene oxide or polyacrylonitrile. The advantages of Li-ion polymer over the lithium-ion design include potentially lower cost of manufacture, adaptability to a wide variety of packaging shapes, reliability, and ruggedness, with the disadvantage of holding less charge. [4]



Figure 3: Lithium Ion Cell

Nickel Metal Hydride (Ni-MH):

The "metal" M in the negative electrode of a NiMH cell is actually an intermetallic compound. Many different compounds have been developed for this application, but those in current use fall into two classes. The most common is AB5, where A is a rare earth mixture of lanthanum, cerium, neodymium, praseodymium and B is nickel, cobalt, manganese, and/or aluminium. Very few cells use higher-capacity negative electrode materials based on AB2 compounds, where A is titanium and/or vanadium and B is zirconium or nickel, modified with chromium, cobalt, iron, and/or manganese, due to the reduced life performances. Any of these compounds serve the same role, reversibly forming a mixture of metal hydride compounds. When overcharged at low rates, oxygen produced at the positive electrode passes through the separator and recombines at the surface of the negative. Hydrogen evolution is suppressed and the charging energy is converted to heat. This process allows NiMH cells to remain sealed in normal operation and to be maintenance-free. [5, 6]



Figure 4: Nickel Metal-Hydride Cell

1.2 Problem Statement

At present, it's a known fact that every battery technology degrades with use and its life reduces. Knowledge on what parameters affect the degradation, which of the parameters influence more among them are still vaguely known. The research highlights the factors which influence the State of Health (SOH) or State of Charge (SOC) of a battery technology. From the series of experiments conducted on the battery technologies, it is evident that the state of health of a battery depends on parameters namely impedance, charging rate(C-Rate), Operating temperature, number of cycles. The extent to which each factor affects is discussed in the results section.

1.3 Scope and Purpose

Irrespective of the battery technology at hand, four different conditions have been maintained for testing the batteries. The four conditions are namely room temperature low charging rate, room temperature high charging rate, high temperature low charging rate, high temperature high charging rate. Nearly seventy to hundred cycles of charging and discharging is being done to study the ageing of the battery over a wide range .It is also due to the fact that the cumulative effects of the parameters averaged over a wide range would provide better test results. Apart from the normal cycling, for every five cycles the impedance is measured because it is the best way to determine state of health of a battery. The primary purpose is to assist in the creation of a portable battery testing device which is under design in a parallel project. Data collected is being used as a lookup table so that the data measured from the tester can be compared with it to determine the remaining life. Also, users and manufacturers of battery chargers can be made aware of the ideal charging rate so that the life of the battery will not be affected.

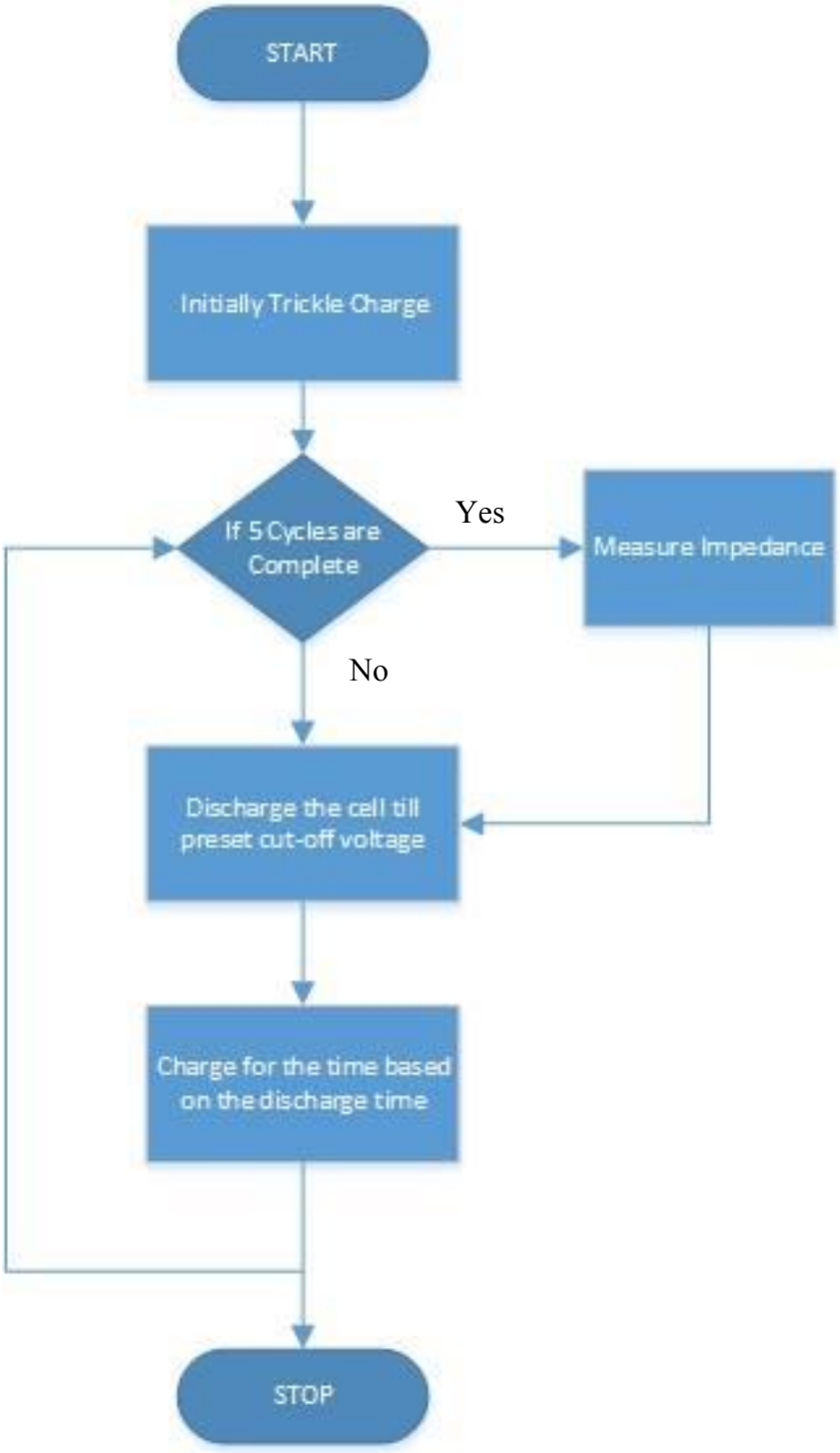

Figure 5: Flowchart for Battery Cycling

CHAPTER TWO

2. LITERATURE REVIEW

2.1 Instruments used

Computerized Battery Analyzer:

Unlike a simple load tester the CBA will test virtually any type or size of battery, any chemistry, any number of cells up to 55 volts. Scientific tests can be easily done on the batteries by letting computer do all the work. The CBA is capable of higher test rates than other testers: up to 40 amps or 150 watts, whichever is higher. It not only tests the total amount of energy stored in a battery (capacity in amp-hrs.), but it graphically displays and charts voltage versus amp-hours. Graphs may be displayed, saved and printed. Multiple graphs of the same battery, or multiple batteries, may be compared or overlaid, a very useful feature. Battery tests may be printed on a color or black and white printer. [7]



Figure 6: Computerized Battery Analyzer

Electronic Load:

Electronic load is a single input programmable DC electronic load. It provides a convenient way to test batteries and DC power supplies. It offers constant current mode, constant resistance mode and constant power mode. The backlight LCD, numerical keypad and

rotary knob make it much easier to use. Up to 10 steps program can be stored. Controlled by PC is also available. It is an essential instrument for design, test and manufacture of many suitable products.

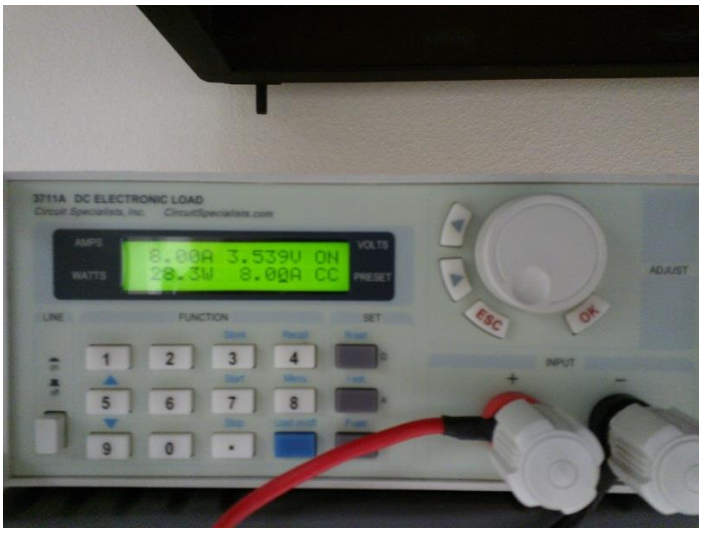

Figure 7: Electronic Load

Potentiostat:

This device is used for measuring the impedance of batteries under test. The device has five leads, two of which goes to positive, two to negative and the other lead is for temperature sensing. It comes with a software Powersuite. Out of the different modes available, the power sine mode is chosen. The frequency over which the data points need to be collected is to be preset. A fraction of the battery EMF (typically 8%) is usually entered as the AC amplitude. Results are interpreted the form of four plots.



Figure 8: Potentiostat

Programmable Power Supply:

Two types of Programmable Power supplies are used to charge the batteries. One is the DC regulated power supply (CSI3010X) and the other is Triple Output DC Power Supply (3631A). The CSI3020X is a regulated linear bench power supply with adjustable current limiting. The LED display shows both Volts & Amps. The current output can be preset by the user via a front panel screwdriver adjustment screw while the voltage is adjustable by a front panel multi-turn knob for precise voltage settings. Output is by front panel banana jacks and there is also a covered terminal strip for remote voltmeter sensing at the load. This bench power supply provides precise output control and allows the end user to pre-set the current output. The ARRAY 3631A is a programmable linear regulated DC power supply. The excellent line and load regulation, extremely low ripple and noise make it well

suited as a high preference power system. The triple power supply delivers 0 to ± 25 V outputs rated at 0 to 1 A and isolated 0 to +6 V output rated at 0 to 5 A. The ±25V power supplies also provide tracking mode to supply operational amplifier and power-amplifying circuit which require symmetrically balanced voltage. Tracking precision is ± (0.2% output +20 mV). The ±25V power supplies can also be used in series as a single 0~50V/1A power supply. [8]



Figure 9: Programmable Power Supply for 8A charging

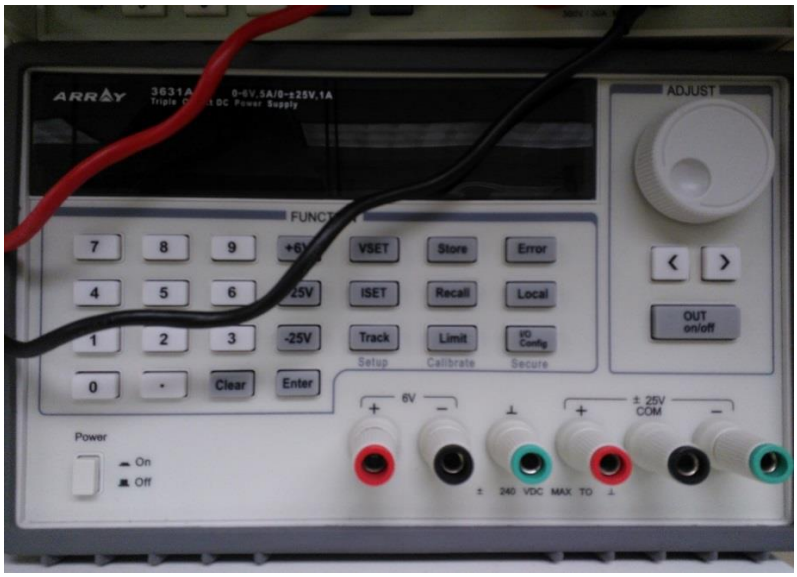

Figure 10 : Programmable Power Supply for 2A Charging

Programmable timers:

Programmable timers are introduced into this project in order to control turn off the supply once the charging time is complete. The main motive is to prevent overcharging of the battery, which comes in handy especially in the absence of users. Two types of timers are being used. One is the Analog daily timer and the other is a Digital weekly timer. The GE 15075 24-Hour Two-Outlet Mechanical Timer is ideal for automatically switching Indoor high wattage loads. This timer allows the user to have up to 48 On/Off times per day which will be separated by a minimum interval of 30 minutes. The built-in manual override allows to disable the scheduled timer and operate the plug-in device(s) with individual On/Off presses on the timer. Hydrofarm's 7 day Digital Program Timer can be programmed for a daily basis, every several days, or several times per day! The timer allows up to 8 on/off times per day, a one minute minimum "on" time, and different settings for different days. The timer is a great way to keep everything on track. Its three prong grounded, has an LCD digital display for easy operation, includes a battery backup, and has a dual outlet feature so you don't lose a plug. These timers are great for lights or hydroponic systems. [9, 10]



Figure 11 : Daily Timer



Figure 12: Weekly Timer

Thermal Chamber:



Figure 13: Thermal Chamber front view

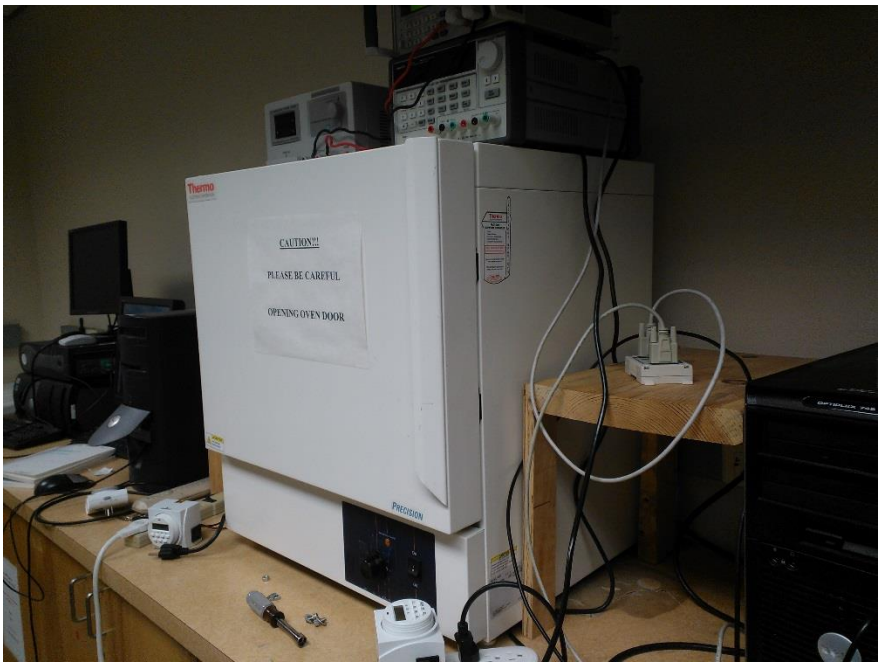

Figure 14: Thermal Chamber Side View

One of the most important component in the research is the Thermal Chamber. Thermal chamber is used to develop high temperature test conditions. The Chamber should be turned on and preheated for some time at the desired temperature. The desired temperature is chosen based on the operating temperature of the battery technology. For a Sealed Lead acid battery, the operating temperature is 60℃ whereas for Lithium-ion batteries the operating temperature is 45℃ . The chamber temperature is monitored with the help of a thermometer inserted at the top. It usually takes ten to fifteen minutes for the chamber to reach the set temperature. Once the set temperature is reached, battery cycling is started. Inside the chamber, there should be utmost care when it comes to handling and placing the battery. The batteries or its terminals should not be kept in such a way that they come into contact with each other. Also it should be kept in mind that the batteries are kept two inches away from the walls of the chamber. For Lithium-ion batteries, there is an extra precaution which needs to be looked into inside the chamber. The setup is shown below.

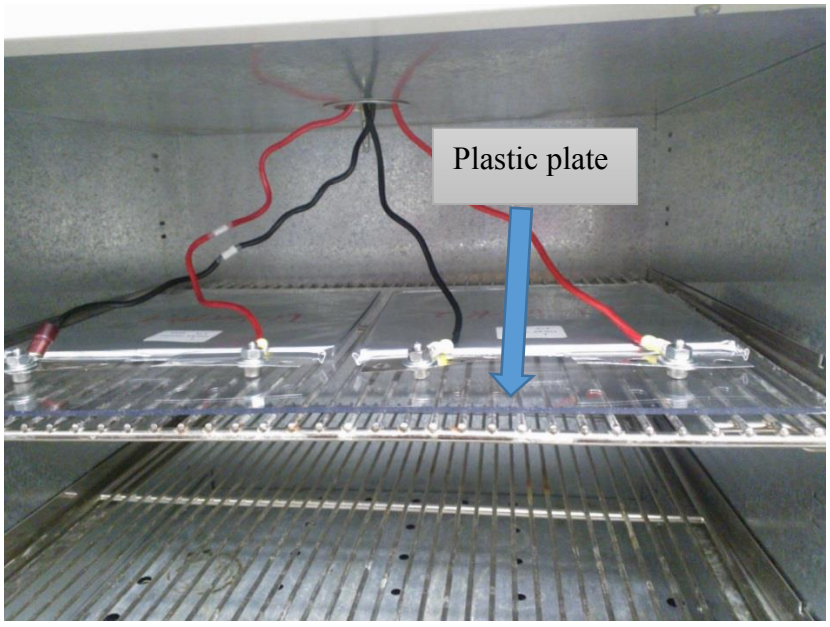

Figure 15: Special base for Li-ion cells inside chamber

In the above setup it can be clearly seen that the battery terminals are wired with the help of metallic screws .These metal screws when in contact with the tray of the chamber short circuits the setup creating thermal run away. In order to prevent this, a plastic plate is placed over the tray, over which the battery is placed.

2.2 Lithium ion Bulging

Of all the battery technologies available in the market, Lithium ion batteries have wide range of applications including portable electronics, hybrid cars etc. Though it has been used in a wide range of applications, one common and most dangerous issue which hasn't been dealt with yet is bulging. Lithium ion bulging is not only a serious issue for the device but also for the user. Lithium being highly inflammable when exposed to air is a matter of concern since it would lead to explosions in the worst case. If not explosion the battery would bulge/ deform which would make it useless for quite some time. The first and foremost reason behind such bulging is overcharging. This usually happens when the battery is not charged with the appropriate charger meant for it. It's the reason why this phenomenon occurs in mobile phones. If instead of a charger, a regulated power supply is used then it should be set in constant current mode with the desired current and the desired time. If the time or current exceeds even by a slight fraction, it can lead to battery bulging. It is also recommended that the regulated power supply is attached to a timer so that it could be monitored in the absence of a person. While operating the timer, it is better to check whether the timer works perfectly before being used. Also, if the wrong time is entered it would also lead to catastrophic results. While conducting the series of tests on Lithium ion batteries, the same thing happened due to the faultiness of the timer. In most of the cases, when this bulging happens, the battery would be rendered useless for few

days. During this period, cycling should be done on the bulged battery, but not through usual means. A flow diagram is depicted below to show the series of experiments which needs to be conducted so as to bring the bulged battery back to its normal working state. [11]

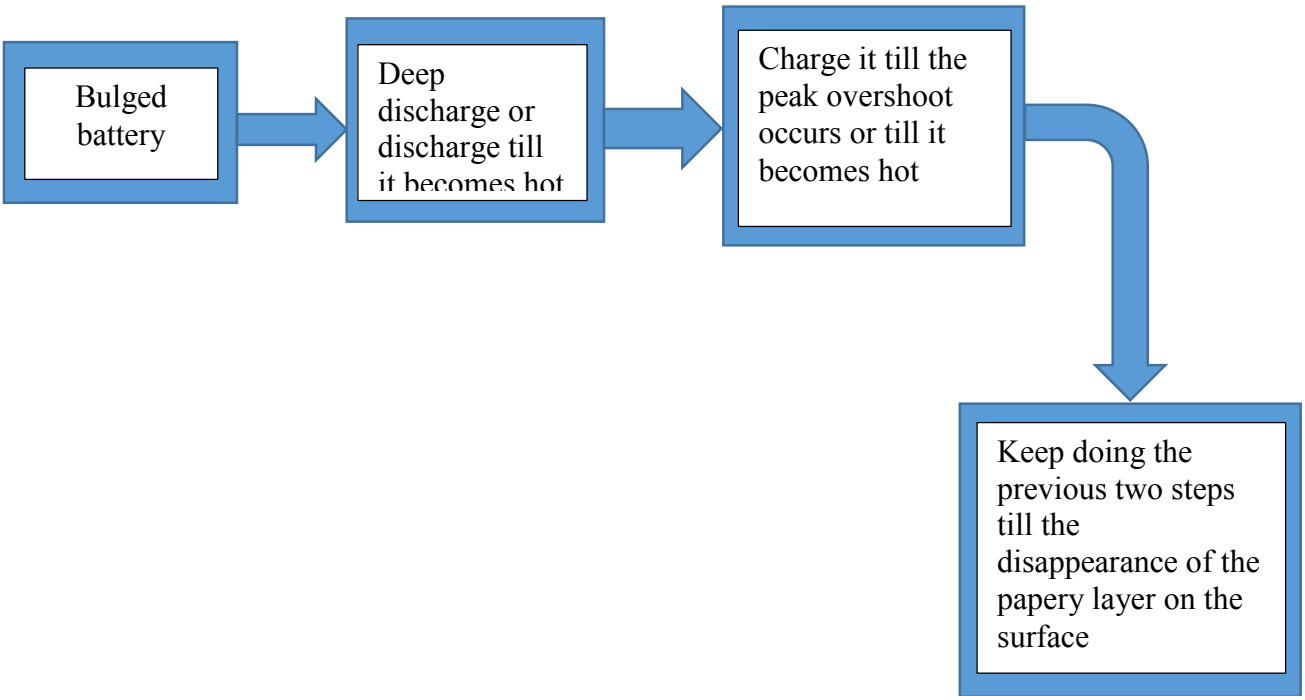

Figure 16 : Flow Chart for Li-ion bulge recovery



Figure 17 : Bulged Cell #3



Figure 18: Bulged Cell #3 (Top View)

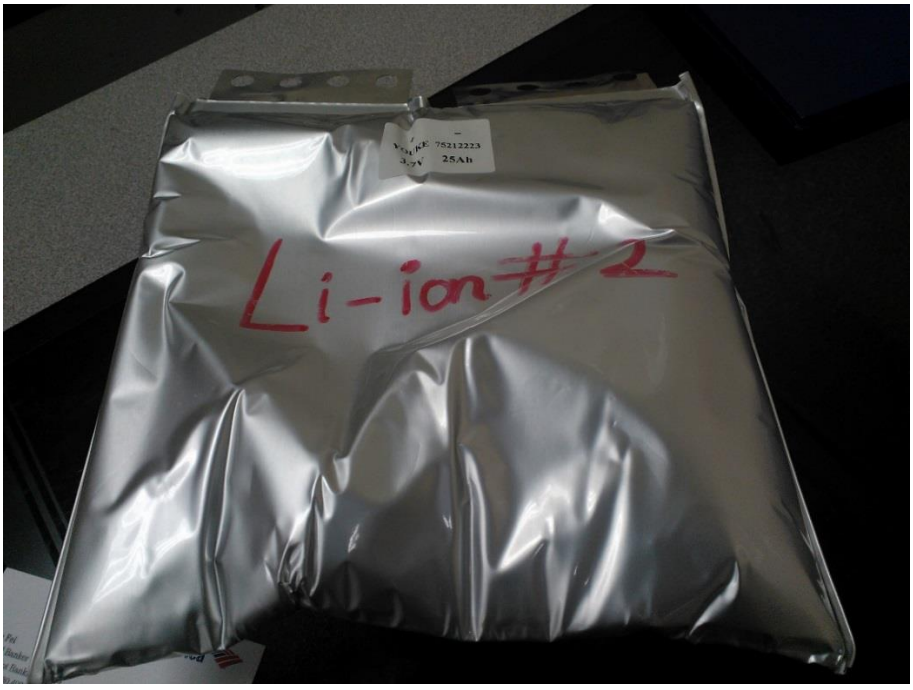

Figure 19: Bulged Cell #2



Figure 20: Bulged Cell #4

Photos above show bulged batteries which deformed during the series of cycling conducted at lab. Major reason for this deformation is due to failure of timers which lead to overcharge of batteries for nearly six to seven hours. The instructions in the flowchart is applicable only when the battery has swollen just one. When it happens for the second time, it cannot be retrieved to its normal conditions. In order to get a better understanding of the battery retrieval process, it is better to discuss the steps in detail. Initially, as mentioned in the flowchart the battery should be deep discharged or discharged till it becomes hot. For this purpose, the programmable electric load should be used instead of the computerized battery analyzer since the latter is not so effective for deep discharging. Once the process is done, the battery is connected to power supply for charging in constant current mode. The battery analyzer is also plugged to the battery terminals at the same time in charge monitor mode, in order to record the Charging curve. The charging curve monitored during one such occasion is shown below.[12]

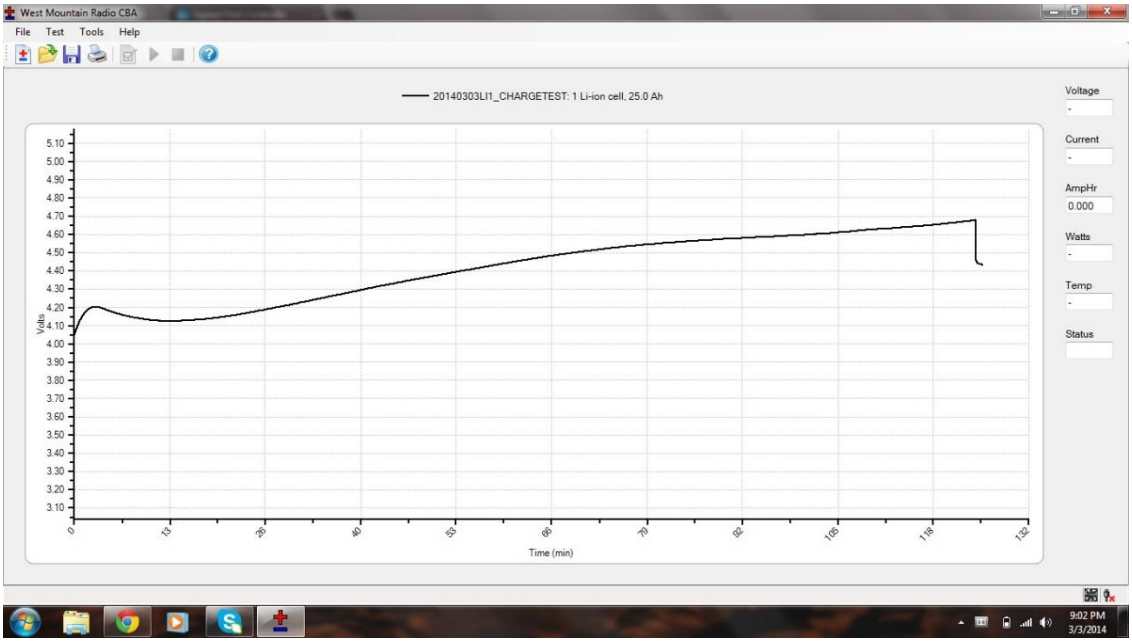

Figure 21: Screenshot of Charging Profile

Once the peak voltage is reached or the battery gets hot, then the charging is stopped. Now it should be checked whether the papery looseness is still present on the surface. If it is still there, then the cycle needs to be carried out till the looseness disappears. Once everything is back in place, the impedance curve is measured just to verify whether the battery is back on track. If there is no problem, then the battery is put back to normal cycling. [13]

CHAPTER THREE

3. METHODOLOGY

3.1 Battery cycling

Initially when the battery is bought, it is recommended that it is put through cycles in order to understand the battery history and the instantaneous capacity. Cycling a battery normally refers to continuous charging and discharging the battery. The time of discharging of a battery is always related to the time of charging during the next cycle. So, it can be inferred that it's a continuous and interdependent process. Once the battery is discharged, the time for the next charging is chosen as either as five or ten percent more than the discharge time. Below is an example to demonstrate the above relationship. [15]

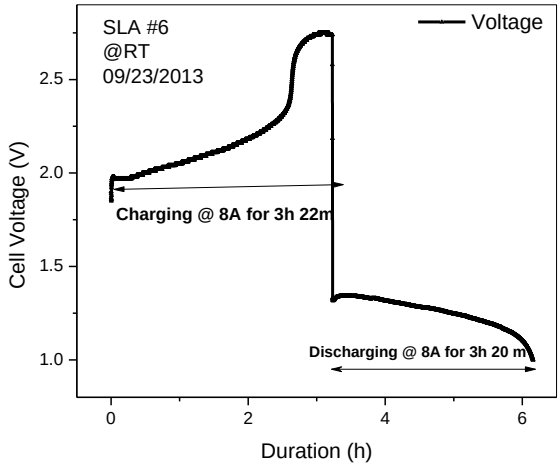

Figure 22: Charge and discharge curve

From the above graph, it can be seen that the discharge time is less than the charge time of the same cycle. This simply means that the charging time of the next cycle is less than the charging time of the previous cycle, indicating degradation in capacity. The time calculated is usually entered in a timer which controls the ON-OFF of a Programmable power supply. The charging can range from 3 hours to even 12 hours depending upon the charging rate

(C-Rate). Based on this a daily schedule has been prepared and strictly followed to make the process uniform and continuous. The graph below denotes the daily schedule for Lithium ion batteries. [16]

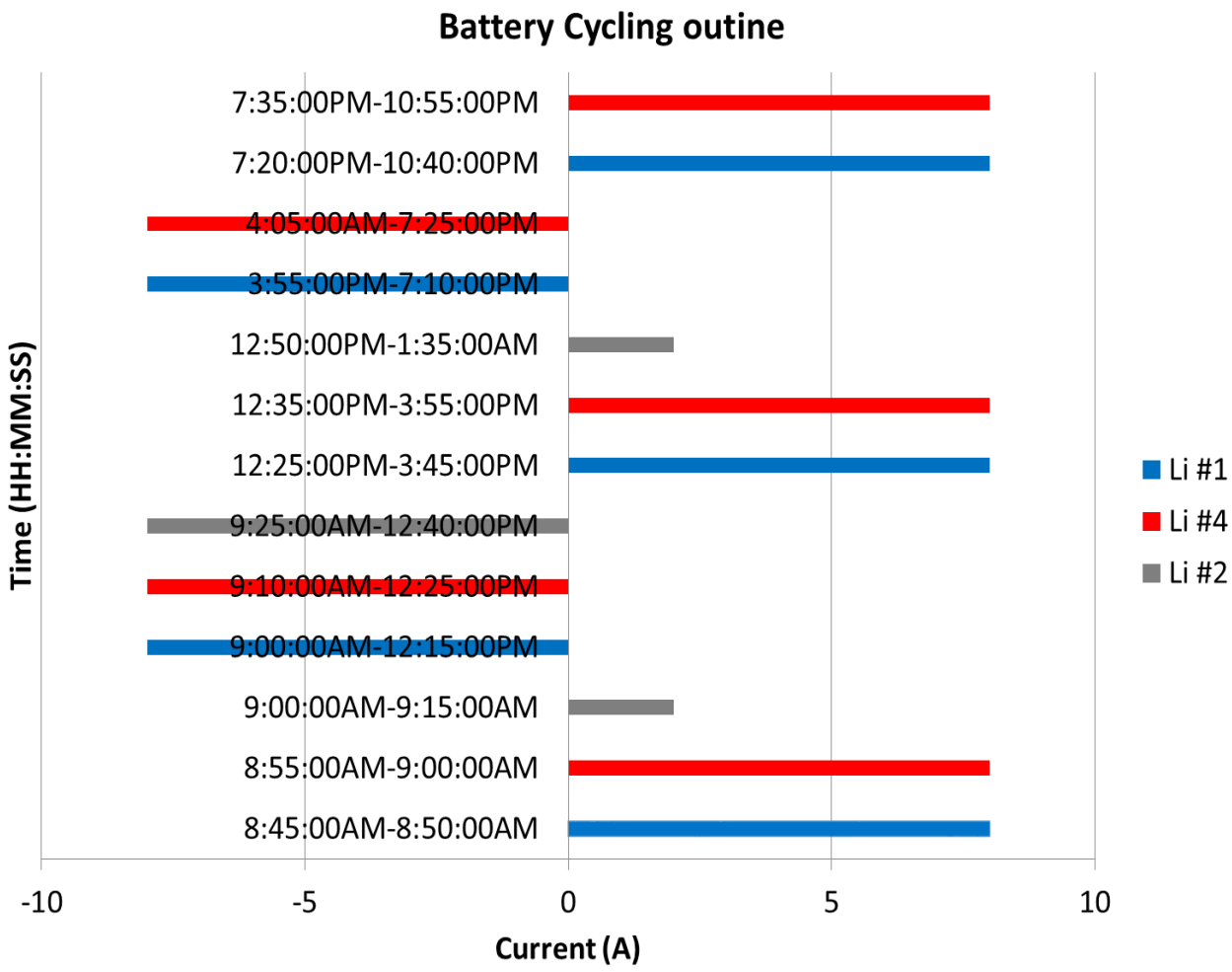

Figure 23 : Daily routine for battery cycling (Li-ion)

In the above graph, the current values denoted by the positive sign denote charging and the ones with the negative sign denote discharging. Li#1 is maintained at room temperature while the others are maintained at high temperature (45 degree Celsius). Li #2 is charged

at 2 A (C/12 rate) whereas the other batteries are charged at 8A (C/8 rate).Irrespective of the temperature and the charging rate, the rate of discharge is always 8 A (C/3 rate). [17]

3.2 Impedance measurement

After five cycles of charging, it is recommended to take measurement of battery impedance. The most commonly followed method for determining the battery impedance is Electrochemical Impedance Spectroscopy (EIS). It is also shown how impedance spectroscopy could bring added value for the improvement of the battery cell design. Continuously measured impedance spectra on half-cells during accelerated ageing tests allow identification of ageing processes and their evolution during lifetime. In addition, impedance spectroscopy as a non-destructive measurement technique provides insights into the battery, which are not available with any other technology. Impedance spectroscopy requires battery-operating conditions to be very precisely defined for the delivery of reproducible results, which might occur under real operating conditions only rarely. Therefore, it is necessary to identify appropriate specific moments for the impedance measurement. The impedance characterization may give better information on the battery's internal capability to perform than the discharge curve directly. In Electrochemical Impedance Spectroscopy EIS a small sinusoidal signal is used to perturb the electrochemical system and the response of the system is observed. The frequency of the signal is varied over a wide range, which makes it possible to monitor processes in the system with different time constants. Furthermore, Impedance spectroscopy has the following advantages. Measurements can be made under real-world operating conditions, e.g., open circuit voltage or under load (DC voltage or current). Multiple parameters can be determined from a single experiment. Relatively simple electrical measurement that can

be automated. Can verify reaction models, and characterize bulk and interfacial properties of the system, e.g., membrane resistance and electrocatalysts. Measurement is non-intrusive – does not substantially remove or disturb the system from its operating condition. A high precision measurement – the data signal can be averaged over time to improve the signal-to-noise ratio. [19, 20]

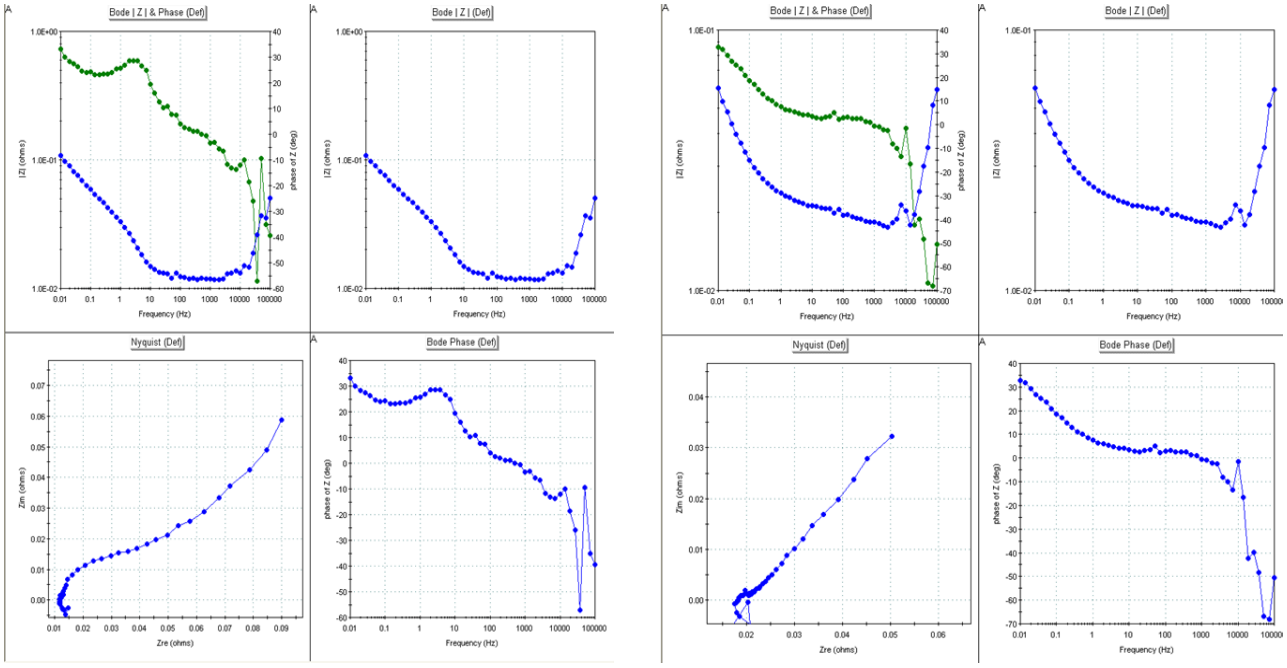

Figure 24: Impedance Spectroscopy output graphs of charged cell and discharged cell respectively.

The graphs above denote the charging and discharging impedance curves respectively. The curves are denoted in the form of four plots namely Nyquist, Bode phase, Bode & Phase plots. While doing data analysis, it is better to consider Nyquist plot for comparative study between the different cycles. This comparative study is an effective way to illustrate the phenomenon of battery ageing as the cycling. The power suite software has an option which allows to export the data to a notepad file from which it can be copied to a data analysis software. Hence, the entire series of nyquist plots in the same graph can be clearly

identified as a display of step by step ageing of a particular battery technology under study. Apart from this plot, the Bode phase plot can also be considered critical for studying the battery impedance and the State of Health determination. If the mouse pointer is moved over the data point at the intersection of the zero on the real axis, the value shown as the modulus of the impedance (Z) is noted .It is commonly referred to as High Frequency Resistance (RHF) and its unit is usually milli-ohm (mΩ). Usually, it is the characteristic of this resistance that it increases with the cycling, which arrives at the obvious conclusion that the State of Health is deteriorating. It is a wrong notion that the RHF value variations depends on the 1electrolyte-conductivity variations. RHF informs on the structure of the PbSO4 layer, and therefore, depends strongly on the history of the previous cycling of the cell. Monitoring the SOC from the single value of RHF was found to be impossible since, for different cycling rates, distinct values of SOC may correspond to the same value of RHF. Fluctuations of RHF were also measured at different SOC: they allow detection of gas evolution in the cell. [21]

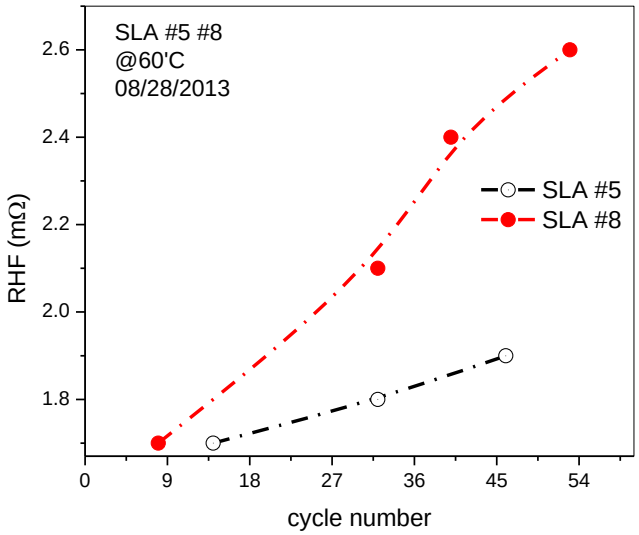

Figure 25: High Frequency Resistance Plot

In the above graph, RHF is shown for two cells maintained at high temperature .If the two curves are observed, it can be clearly seen that there is more slope for SLA #8 compared to that of SLA #5. The reasons for such increase is being discussed in the forthcoming sections.

The experimental setup and procedure is now being discussed.

- Before connecting the leads of potentiostat to the battery terminals, the voltage of the battery should be measured.
- Now the battery is connected to the leads. One must make sure that the terminals are not interchanged as it would trigger the effect of thermal runaway. The connection changes for batteries and fuel cells. For batteries the green lead which comes along with the white lead is given to positive terminal and the red lead is given to the negative terminal. Its totally the other way round for fuel cells.
- Once this setup is complete, the software "Power Suite" is opened. The device is now turned on and after a five to ten second gap, the Cell Enable button is turned on.
- Choose **Experiment →New**. The dialogue shown below automatically pops up.

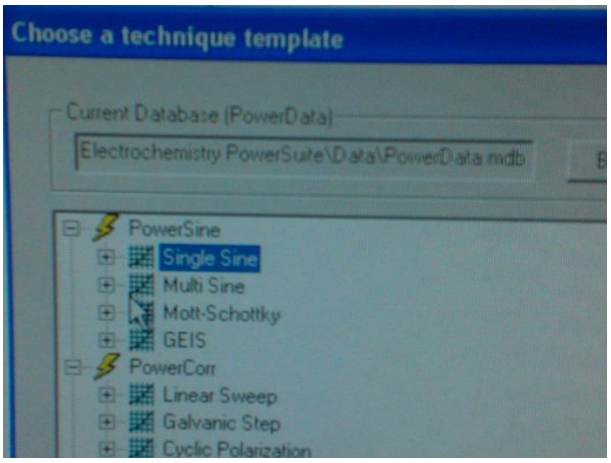

Figure 26 : Screenshot #1 of Powersuite dialog box

The Single Sine template is chosen under the Power Sine mode for the desired test results. For techniques other than impedance spectroscopy, other available modes are chosen.

- Under the Single Sine mode there are a number of user defined templates out of which SRP Experiment template is chosen and given a unique name under which the graphical results will be saved.

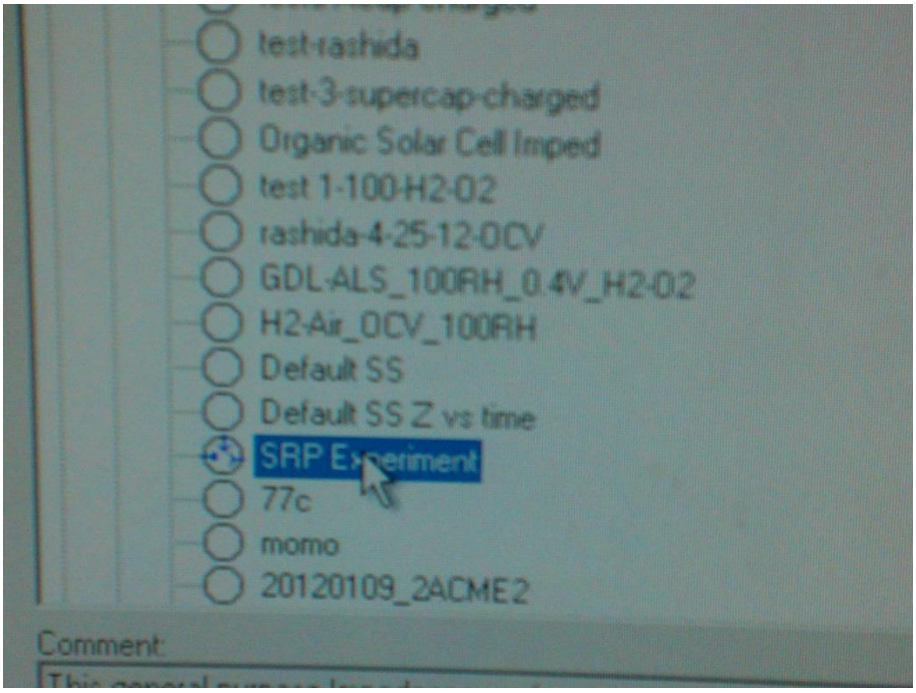

Figure 27: Screenshot #2 of Powersuite dialog box

- The next two dialog boxes which pop up need to be left default and skipped to the next dialogue where critical setting is to be done.
- In this dialog, the start and the end frequencies are first given to denote the range over which data points are to be collected. A broad range of data collection over the wide frequency range can be very useful from the analysis and result point of view. But if time is also considered a perspective, it's not a good idea to have a broad range of frequencies. It is recommended that the start frequency is given 100

kHz and the end frequency is given 10 mHz so that the process is somewhat less time consuming and at the same time arrives at desired results.

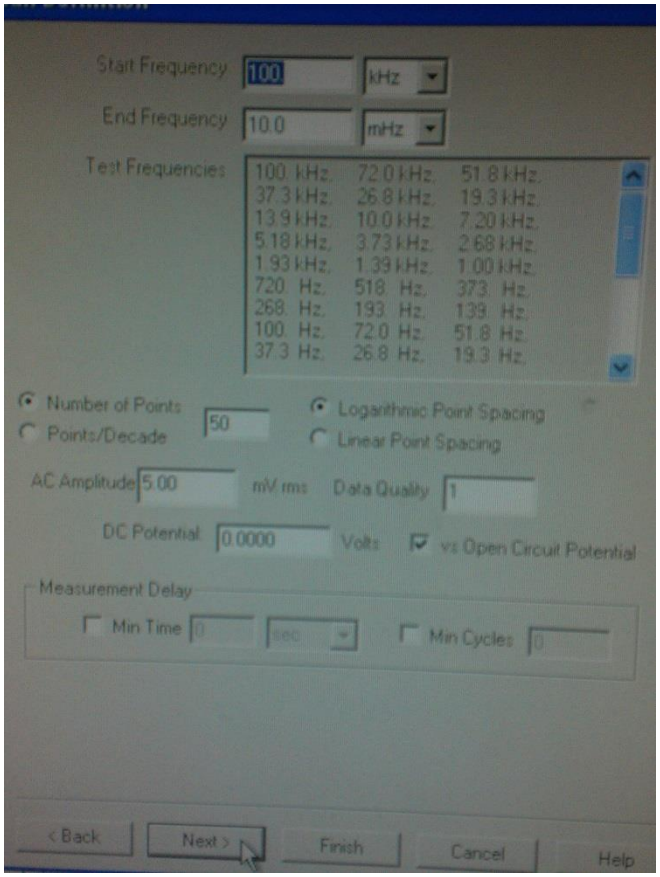

Figure 28: Screenshot #3 of Powersuite dialog box

Once the frequency has been set been set, the next thing to look for is the AC amplitude. The AC amplitude decides smoothness of the plots. A fraction or percentage of the cell voltage is usually entered as the AC amplitude. Based on the series of experiments conducted, it has been found that the ideal percentage of the cell voltage for a best curve fitting is eight. This value is entered as the AC amplitude and the next button is pressed.

- In the final dialog screen which appears along with the result, the option “External Cell” is chosen and the process starts. In order to find the High frequency resistance (RHF) the mouse pointer is moved over the data point over the zero line. The

experiment is paused, all the data points are erased and is again started in order to account for repeatability. This is done four to five times after which the RHF value is noted.

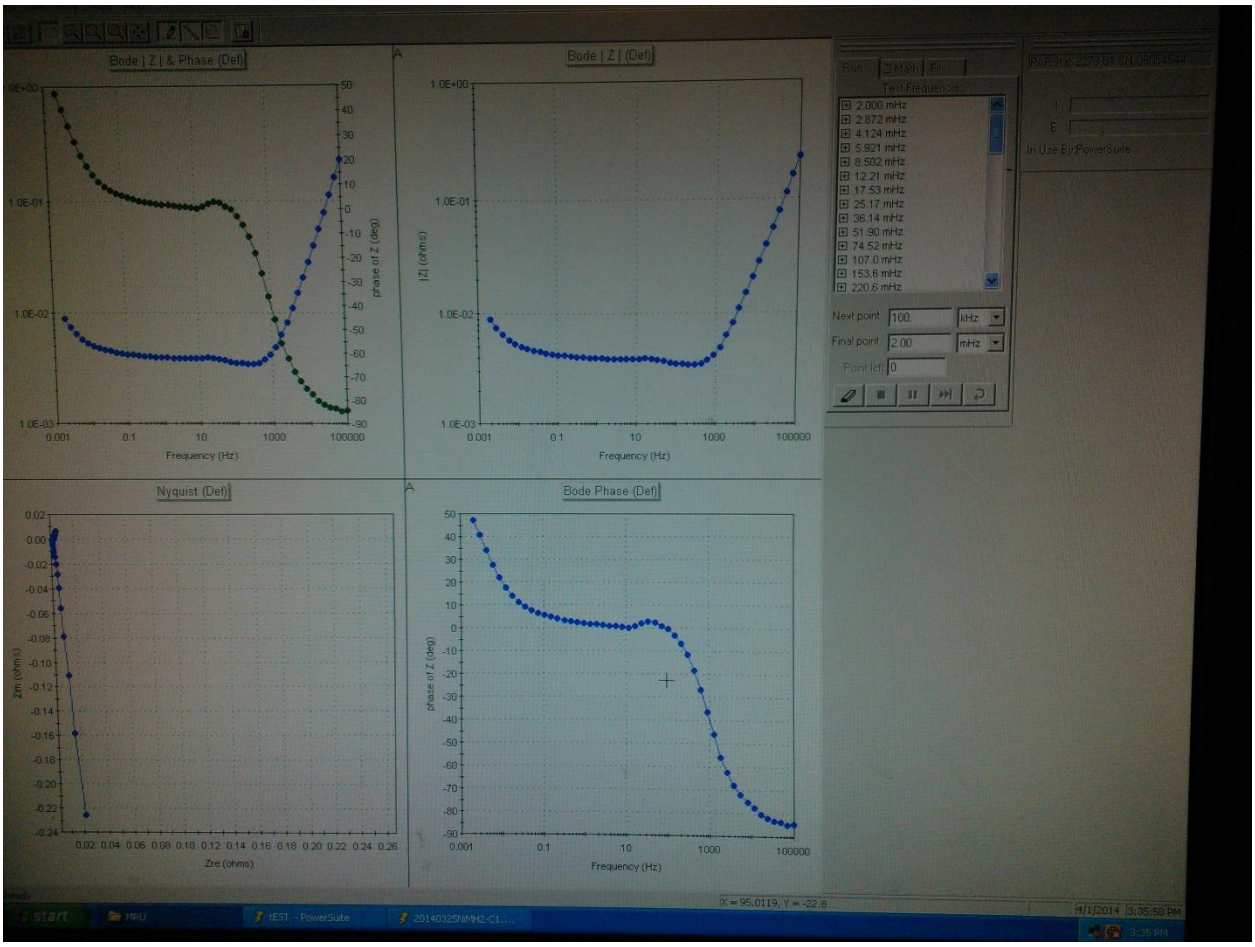

Figure 29: Screenshot of Impedance spectroscopy output graphs of a charged lead acid cell

- Finally the plots obtained are saved and the data can be exported to a notepad file. In order to do so, the individual plots should be selected, exported separately and then saved.

3.3 Regression Analysis

Apart from the various scientific methods to determine the influence of battery parameters in the State of Health of the battery, it is better to perform a mathematical model to cross check whether it correlates with the methods. Regression analysis is a statistical technique for investigating and modeling the relationship between variables. [18] It is denoted by the equation

$$y = \beta 0 + \beta 1 x + \varepsilon$$

Where, y – dependent (response) variable

x – Independent (regressor/predictor) variable

β0 – intercept

β1 - slope

ε - random error term

Multiple linear regressions are extensions of simple linear regression with more than one dependent variables. A multiple regression model that might describe this relationship is given by the equation

$$y = \beta_0 + \beta_1 x_1 + \beta_2 x_2 + \varepsilon$$

The above equation shows multiple linear regression of the order 2. If the model is of order k, then the equation will go on till$\beta_k x_k$. One of the important methods of analysis used under multiple linear regression is the model adequacy check. In order to understand this clearly, three models have been discussed .Each model under adequacy check is denoted by four plots, based on which conclusions have been drawn. [18]

Normal Probability Plot: It is important that the normality plot is close to the normality line, without skewedness and tailed distribution. If any of the two is present, it indicates a

problem with normality. The full model shows light tailed distribution as shown in Figure 3 .The subset model 1 shown in Figure 4 is not a continuous plot and so normality is a problem here as well. In case of Figure 5, there is no problem with normality since the plot is very close to the normality line.

Versus Fit: They are mainly useful in detecting the common types of model inadequacies. If this plot resembles a particular pattern, it indicates model deficiencies. Based on the observation of the plots of three models, we can conclude that they do not exhibit any pattern. In other words there is no deficiency in all the models.

Histogram: If we compare all the three models, we find a problem at the tail for first two models whereas for the third model it seems that there is no problem.

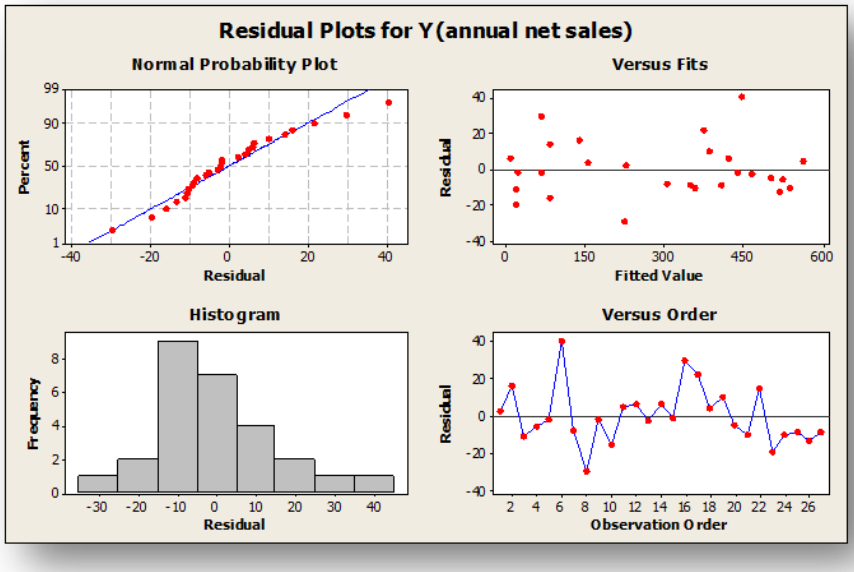

Figure 30: Sample Residual plot #1

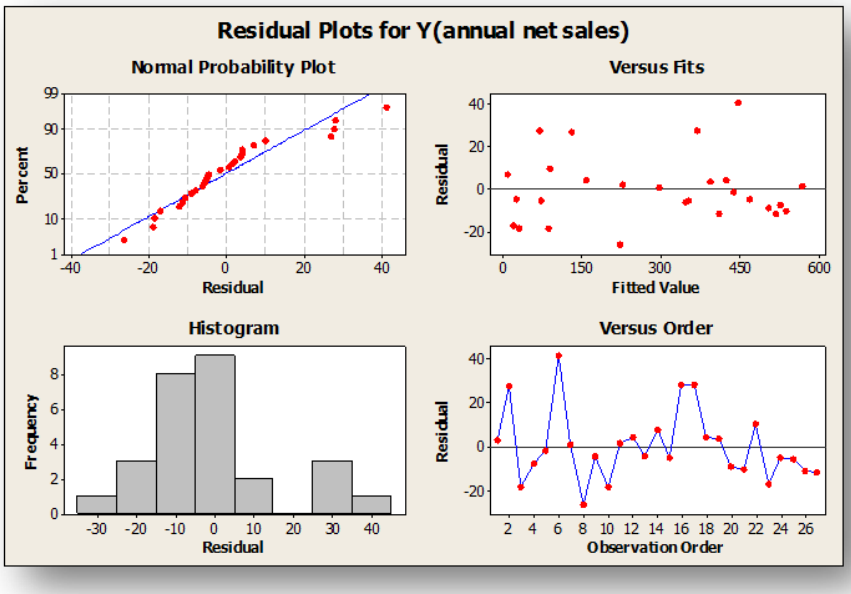

Figure 31 :Sample Residual Plot #2

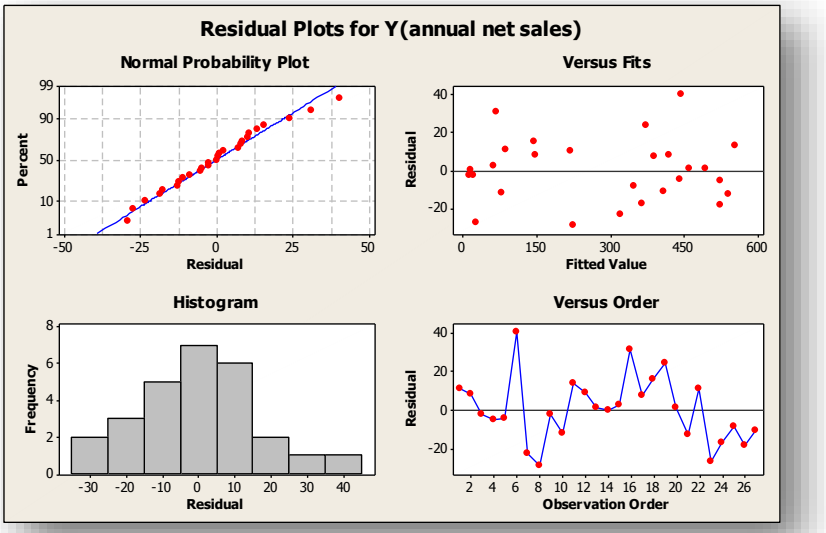

Figure 32: Sample Residual Plot #3

CHAPTER FOUR

4. RESULTS

4.1 Mathematical Analysis

As discussed earlier, the mathematical analysis through multiple linear regression is being used. It is being used to arrive at a mathematical equation involving the response Battery capacity and some predictors namely impedance, temperature and charging rate. Another equation is also being derived, which relates the response Impedance to various predictors namely charging rate, Temperature, number of cycles, interaction term between cycle number and temperature, interaction term between cycle number and charging rate. Screenshots below denote the Minitab worksheets which are being used to derive equations for Battery Capacity and Impedance.

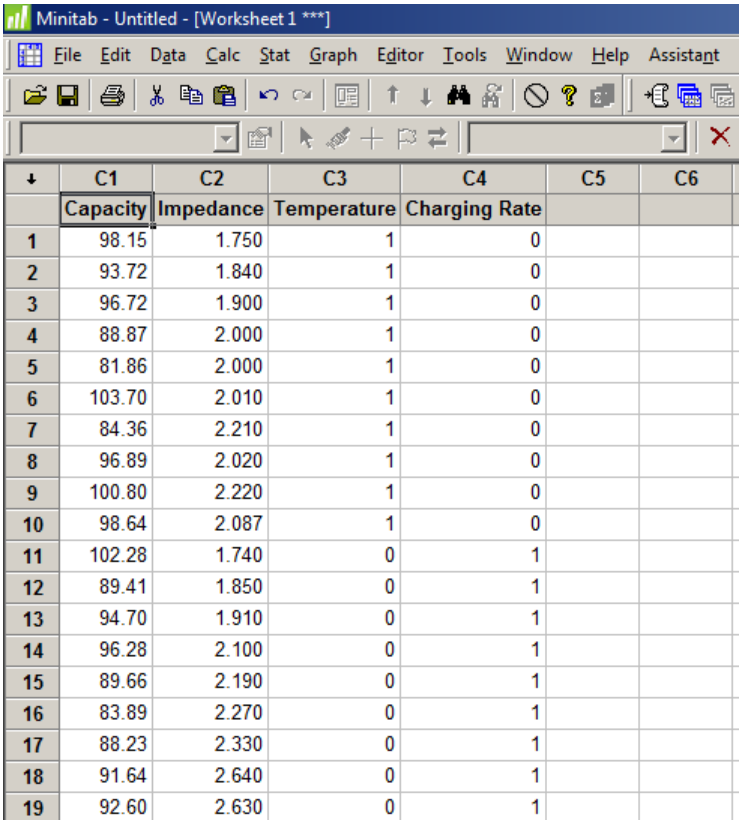

	C1	C2	C3	C4	C5	C6
	Capacity	Impedance	Temperature	Charging Rate		
1	98.15	1.750	1	0		
2	93.72	1.840	1	0		
3	96.72	1.900	1	0		
4	88.87	2.000	1	0		
5	81.86	2.000	1	0		
6	103.70	2.010	1	0		
7	84.36	2.210	1	0		
8	96.89	2.020	1	0		
9	100.80	2.220	1	0		
10	98.64	2.087	1	0		
11	102.28	1.740	0	1		
12	89.41	1.850	0	1		
13	94.70	1.910	0	1		
14	96.28	2.100	0	1		
15	89.66	2.190	0	1		
16	83.89	2.270	0	1		
17	88.23	2.330	0	1		
18	91.64	2.640	0	1		
19	92.60	2.630	0	1		

Figure 33: Screenshot of Minitab Worksheet #1

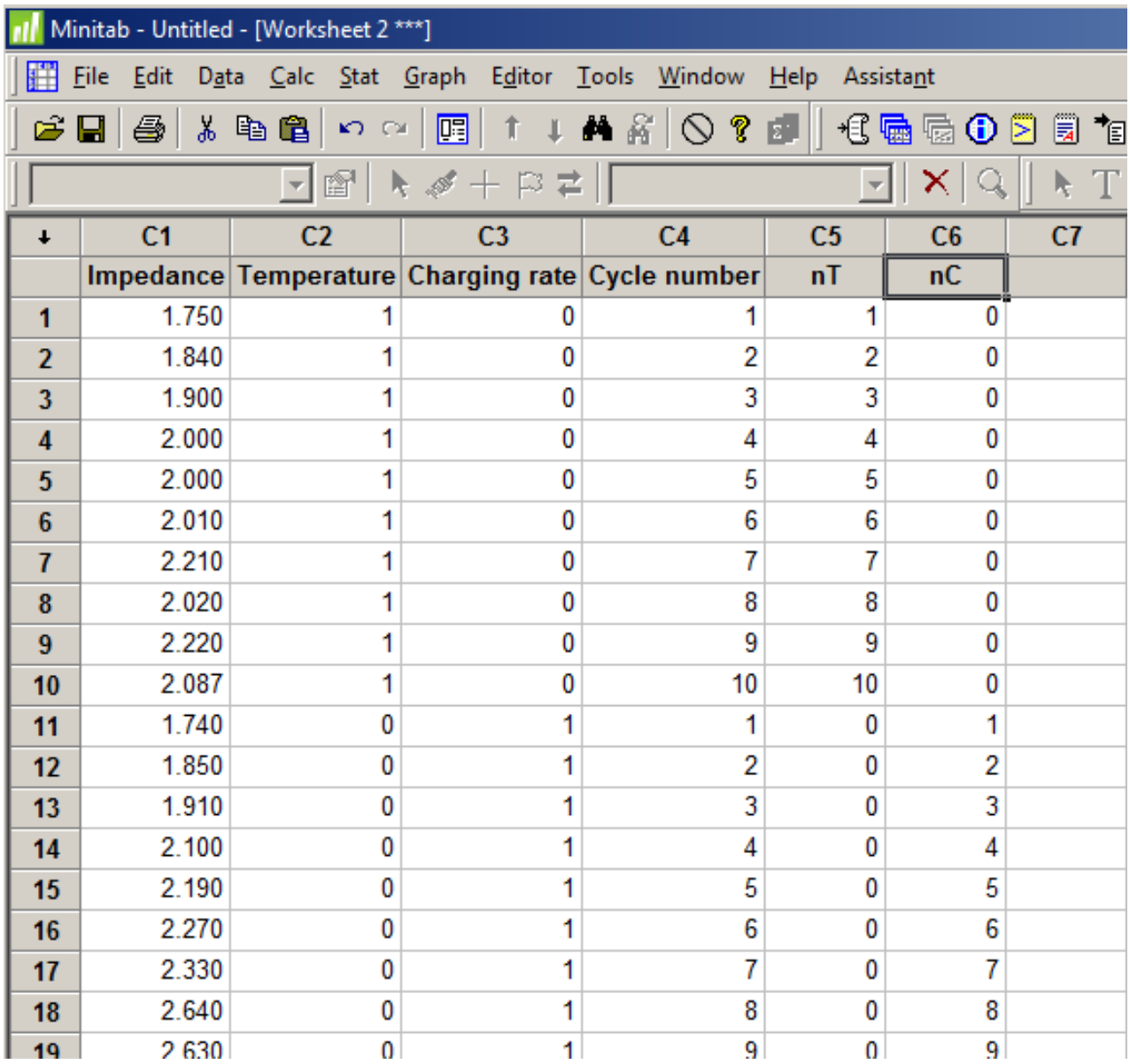

↓	C1	C2	C3	C4	C5	C6	C7
	Impedance	Temperature	Charging rate	Cycle number	nT	nC	
1	1.750	1	0	1	1	0	
2	1.840	1	0	2	2	0	
3	1.900	1	0	3	3	0	
4	2.000	1	0	4	4	0	
5	2.000	1	0	5	5	0	
6	2.010	1	0	6	6	0	
7	2.210	1	0	7	7	0	
8	2.020	1	0	8	8	0	
9	2.220	1	0	9	9	0	
10	2.087	1	0	10	10	0	
11	1.740	0	1	1	0	1	
12	1.850	0	1	2	0	2	
13	1.910	0	1	3	0	3	
14	2.100	0	1	4	0	4	
15	2.190	0	1	5	0	5	
16	2.270	0	1	6	0	6	
17	2.330	0	1	7	0	7	
18	2.640	0	1	8	0	8	
19	2.630	0	1	9	0	9	

Figure 34: Screenshot of Minitab Worksheet #2

Once the data is being entered, the Stat button on the toolbar is chosen under which Regression is chosen from another option under the same name.

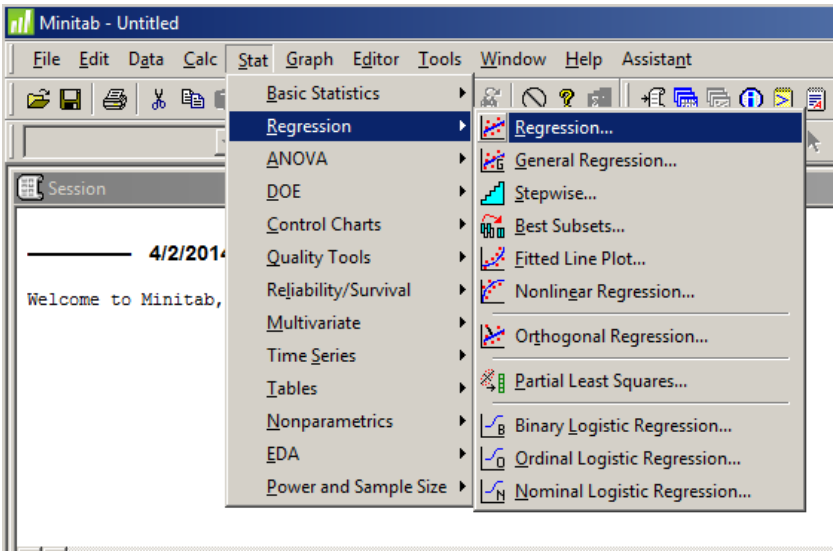

Figure 35: Screenshot of Minitab Toolbar

Under the response dialogue, Capacity is entered whereas Impedance, Temperature and charging rate are entered in the predictors dialogue box. "Graphs" button is chosen under which "four graphs in one option" is chosen. Under "Results" button the option which has regression equation is chosen. Variance Inflation Factors are chosen under the "Options" button.

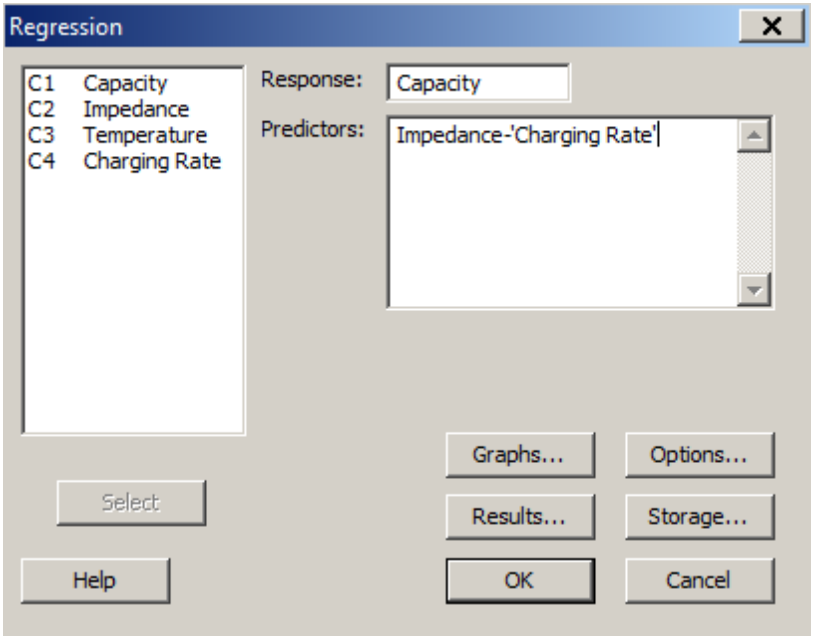

Figure 36: Screenshot of Minitab dialog box #1

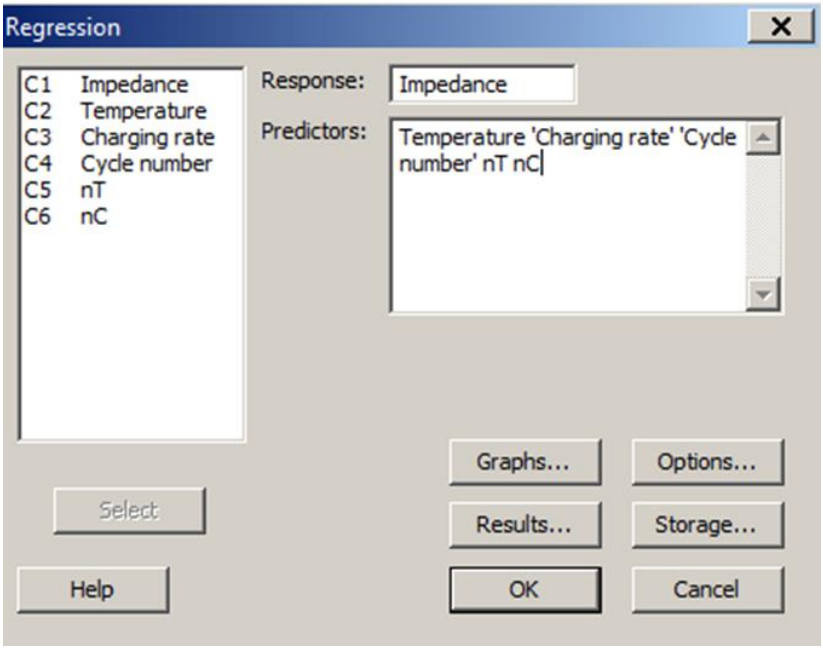

Figure 37: Screenshot of Minitab dialog box #2

Once the OK button is pressed, a dialog displaying the results of the regression analysis as well as the residual plots are obtained. Studies should be made on the results in order to evaluate the two process. The main focus of this analysis is to study how the process is performing. That is, whether the process is in concordance with the normality or not. Firstly, the results of the regression dialogue box are compared. The regression equation for capacity has only one negative term. Also, the Variance Inflation Factors are nearly one .Both these indicate the fact that the presence of Multicollinearity is very less in the process. In order to get a better understanding of the regression equation, it would be better if the batteries are analyzed separately. After the analysis, we can arrive at the conclusion that for a battery with high charging rate and high temperature conditions, the charging rate has a slightly higher impact on the capacity than temperature. This arrives at an overall conclusion that the Charging rate has a high impact on the capacity

Welcome to Minitab, press F1 for help.

General Regression Analysis: Capacity versus Impedance, Temperature, ...

Regression Equation

Capacity = 106.298 - 11.1743 Impedance + 10.2343 Temperature + 11.0696 Charging Rate

Coefficients

Term	Coef	SE Coef	T	P	VIF
Constant	106.298	3.55322	29.9160	0.000	
Impedance	-11.174	1.70950	-6.5366	0.000	1.69278
Temperature	10.234	1.89959	5.3876	0.000	1.14854
Charging Rate	11.070	2.20583	5.0183	0.000	1.52451

Figure 38: Screenshot of Minitab result #1

The Regression equation for impedance is now considered for analysis. There is no alternative positive and negative sign in the regression equation which doesn't indicate multicollinearity. Variance Inflation Factors are less than 10, which indicates the presence of only moderate multicollinearity. The R-Sq value is approximately 89% and the adjusted R-Sq value 87 % which indicates the approximate variability in the process.

Welcome to Minitab, press F1 for help.

Regression Analysis: Impedance versus Temperature, Charging rate, ...

The regression equation is
Impedance = 1.69 + 0.027 Temperature + 0.022 Charging rate + 0.0359 Cycle number
+ 0.0518 nT + 0.0868 nC

Predictor	Coef	SE Coef	T	P	VIF
Constant	1.6940	0.1307	12.96	0.000	
Temperature	0.0274	0.1425	0.19	0.848	4.344
Charging rate	0.0216	0.1473	0.15	0.884	4.569
Cycle number	0.03593	0.01898	1.89	0.065	4.057
nT	0.05179	0.01903	2.72	0.009	5.594
nC	0.08679	0.02082	4.17	0.000	7.986

S = 0.236830 R-Sq = 89.2% R-Sq(adj) = 87.9%

Analysis of Variance

Source	DF	SS	MS	F	P
Regression	5	19.4826	3.8965	69.47	0.000
Residual Error	42	2.3557	0.0561		
Total	47	21.8383			

Figure 39: Screenshot of Minitab result #2

The same logic which was applied to the capacity analysis is now applied to the Impedance equation. Now, if the batteries are considered individually and analyzed, it can be observed that the charging rate and temperature have nearly the same effect on the impedance. However if the interaction with the effect of cycling is considered, the charging rate along with cycle number has more effect on the impedance than the combined effect of temperature and cycle number. Hence, it can be concluded from the analysis of regression that the charging rate has more influence on the impedance and hence the capacity of a battery.

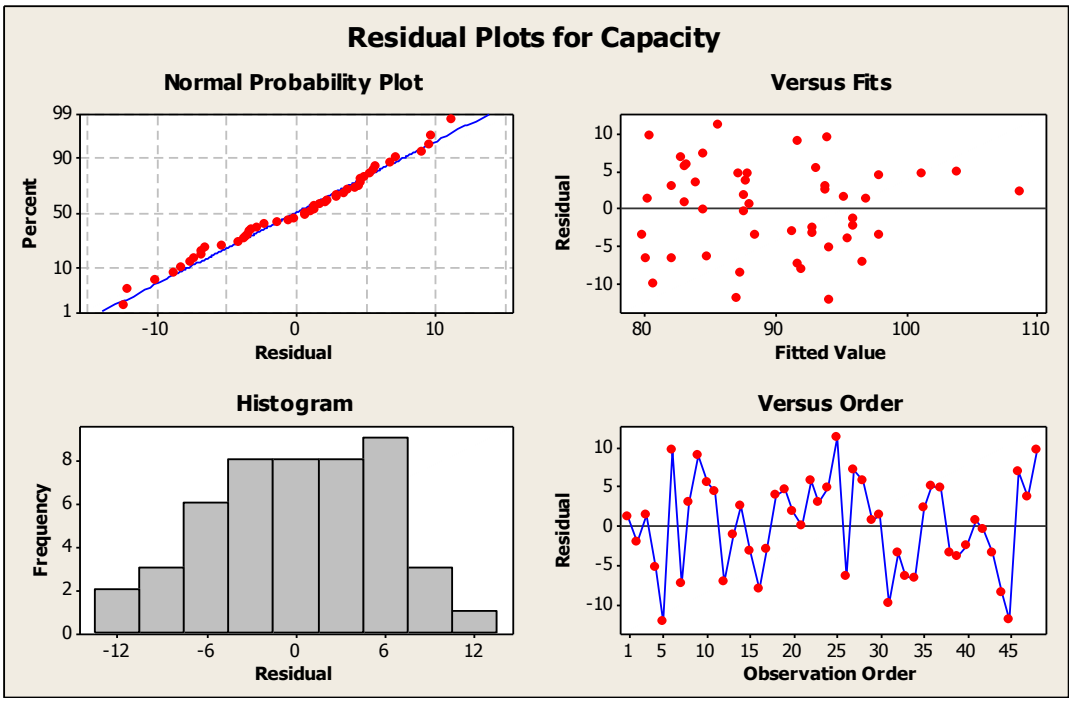

Figure 40 : Residual Plot of Capacity

Analysis of residual plots is usually done in order to perform model deficiencies. Four plots are discussed in detail so that the occurrences or the ways to find out model deficiencies could be understood easily. Firstly, the normal probability is considered .It is recommended that the normal probability plots should not have a heavily tailed error distribution. It is because such distribution tends to shift the least squares fit too much in that direction which would require complex estimation techniques. The normal probability plot in the above figure has "idealized" normal probability plot since all the points lie along a straight line. This indicates that there is no significant deficiency in the model. Now, versus fit is taken for analysis. It's a fact that if the dataset doesn't form any pattern such as funnel, double bow or non-linear then it is considered a satisfactory plot. In the above versus fit plot, it can be clearly seen that the entire dataset can be fit in a horizontal band. So there is no inadequacy issue with the model. Then comes the Histogram.

It is important that the peak occurs close to the center. Deviation from the center indicates model inadequacy. In the given histogram, the peak is skewed to the right by six units which indicates model inadequacy. In the versus order plot, the key criteria to look out for is autocorrelation. Positive autocorrelation is the condition when a series of points follow a specific trend either upwards or downwards and then in the opposite direction for nearly the same length in the opposite direction. On the other hand, negative correlation is the case when the adjacent data points come in a zigzag pattern above and below the zero line. The presence of auto-correlation in the errors is a huge violation of basic assumptions. Here it can be seen that the plot doesn't have any autocorrelation which suggests that there is no inadequacies.

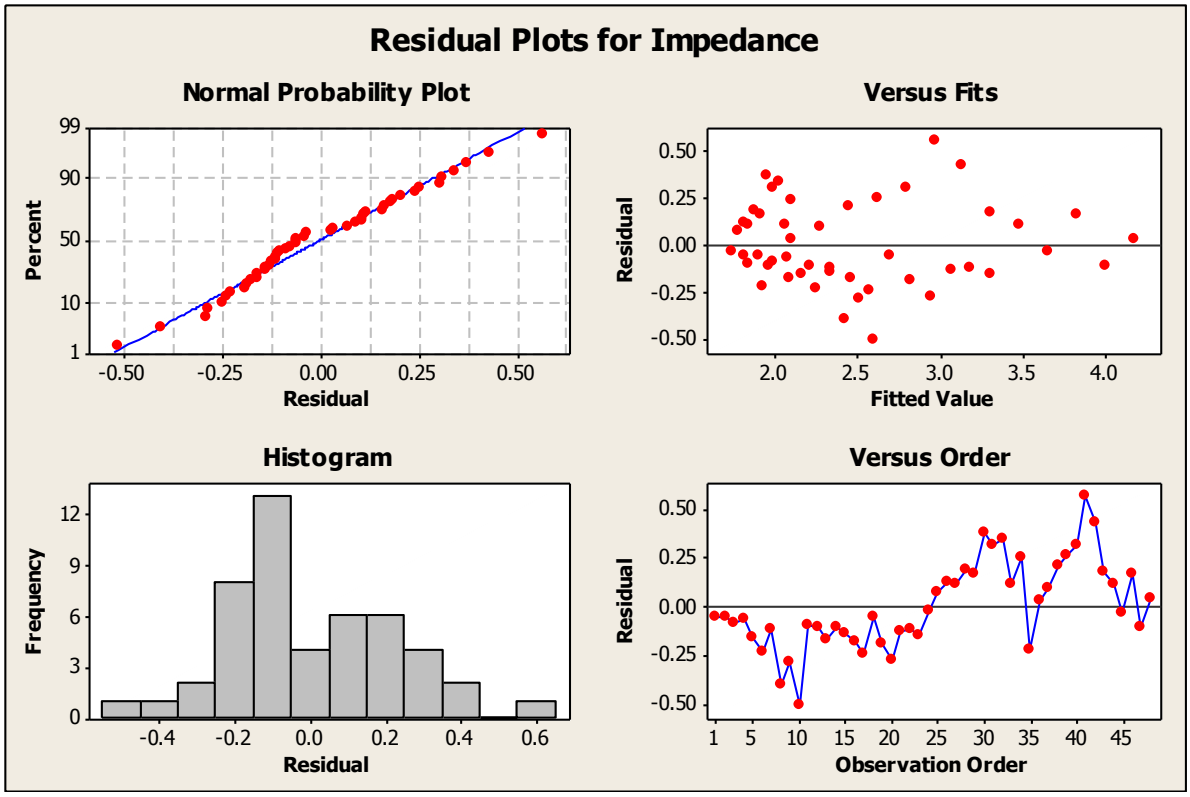

Figure 41: Residual Plot of Impedance

The same analysis is performed on the residual plot for impedance. The normality curve does not appear to be as perfect as that for capacity but it is linear. Versus fit plot shows

that it has a funnel shaped pattern. This indicates a sign of inadequacy due to the presence of non-constant variance. The histogram doesn't have much problem since there is only a slight deviation from the center. Finally versus order graph is taken into consideration. It appears to have positive autocorrelation which is a serious issue and requires special statistical tests for detecting and dealing with it. Based on the analysis of the two residual plots it is clear that the model which relates the battery capacity to impedance is better than the one built with impedance alone. Thus analyzing a battery's capacity or state of health with respect to impedance is the best approach. [18]

4.2 Discharge curves

Sealed lead Acid Batteries:

The batteries which are being used for cycling are 2 V, 25 Ah batteries. Initially, they are being cycled at room temperature and low charging rate (C/12) in order to get them tuned and reach a good initial capacity. Once they do so, they are maintained at four different conditions as shown below

Table 1: Sealed Lead Acid Battery conditions

Sealed Lead Acid battery number	Charging rate	Temperature
#1	2A (C/12)	Room Temp.
#2	8A (C/3)	Room Temp.
#3	2A (C/12)	High Temp.
#4	8A (C/3)	High Temp.

However the discharge rate is maintained the same for all batteries (C/3 rate) irrespective of the charging rate and temperature. The charge input was fixed at 105 % of the previous

discharge capacity values for the cells at high C rate and at 110% of the previous discharge capacity values for the cells at low C rate. Graphs below show the discharge profiles for all four cells #1, 2, 3 and 4, respectively at C/3 discharge rate both at initial and final cycle numbers

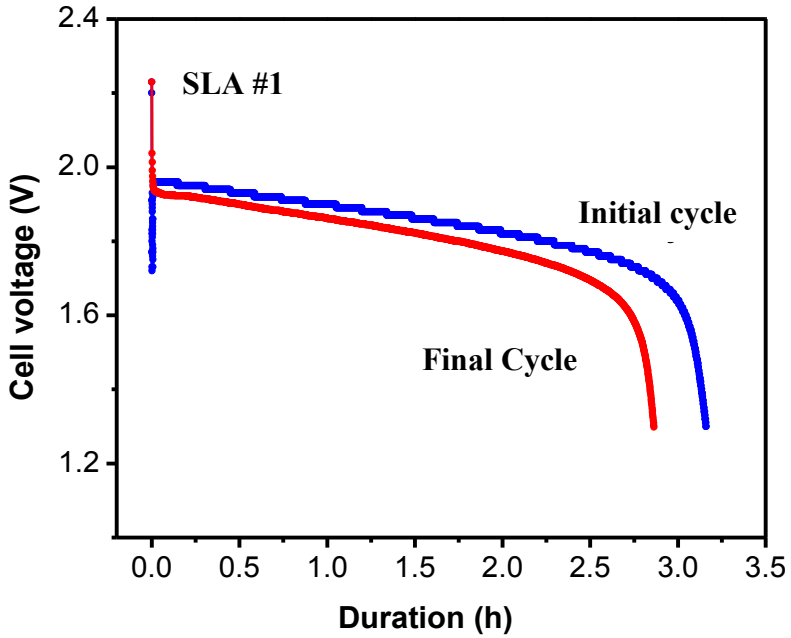

Figure 42: Discharge Profile of Lead Acid Cell #1

For cell #1, the initial discharge capacity is measured after five to six initial tuning cycles. Data is exported to a notepad or excel file, from which the data is copied to a statistical data analysis software. The software used here is Origin. Once this data is collected, the cell is put to normal cycling with impedance measurements for every five cycles. Since the cell is charged at a slower rate, it is possible to cover approximately seventy cycles. At the end of seventieth cycle the final discharge curve is exported and plotted in the same manner. Now the initial and final discharge curves are compared. It can be clearly seen by looking at the graph that the final discharge cycle curve falls before the initial discharge

curve. This is because of the reduction in the discharge time which clearly denotes the rate at which the cell degrades. [21, 22]

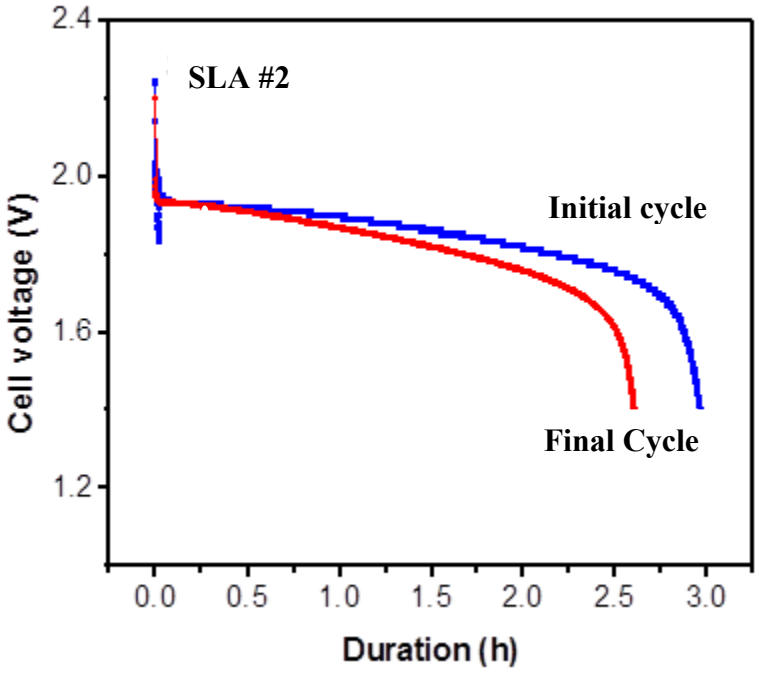

Figure 43: Discharge Profile of Lead Acid Cell #2

Cell #2 is maintained at the same temperature condition as cell #1. But the only difference is that the rate at which this cell is charged is faster. The initial discharge curve is plotted in the same manner as before .Since the charging rate is faster, there is a scope for more number of cycles to be carried out. Nearly hundred cycles have been done for this cell. At the end of cycling, the final discharge curve is collected and plotted. When these two curves are taken and compared, the final discharge curve falls short in a similar fashion. But when compared to the previous cell, the final discharge curve falls shorter for the latter than the former cell. This clearly indicates the fact that the degradation in the second cell is more which can be attributed to the no of cycles and at the same time to the rate at which the cell is being charged. [23, 24]

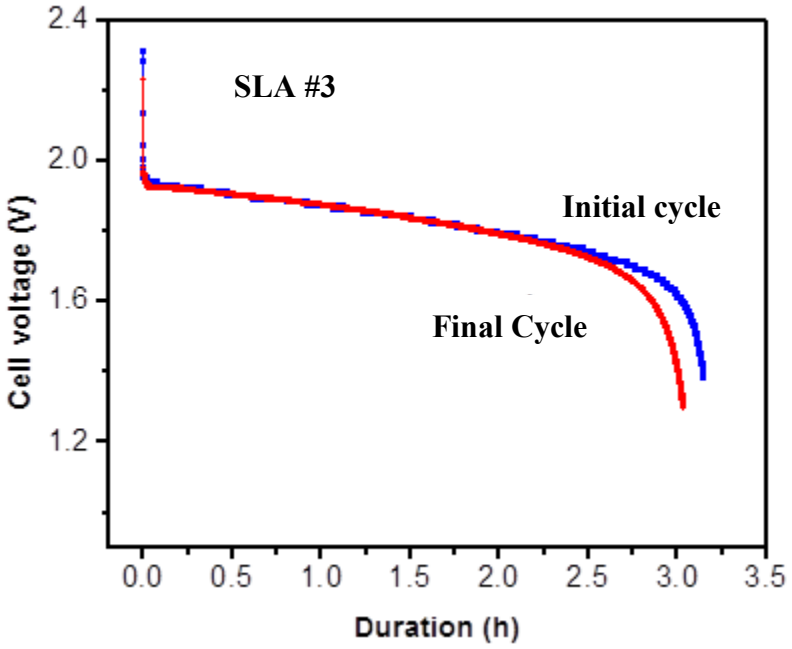

Figure 44: Discharge Profile of Lead Acid Cell #3

Cell #3 represents the slow charging rate (C/12) condition which is same as that of Cell #1.But the difference is that it is maintained at high temperature. Similar to Cell number #1 the initial discharge curve is obtained and since the rate of charging is slow, the number of cycles which could be completed is nearly seventy. Impedance measurement is also being done every five cycles. Once seventy cycles have been completed, the discharge graph for the seventieth cycle is exported and is plotted along with the initial discharge curve in Origin. When they are put together and compared, the final discharge curve falls behind as usual .When compared to cell #2, the degradation is less whereas for cell #1 there is only slight difference. This indicates that the influence of charging rate is more than that of temperature. However the combined effect of both temperature and charging rate should be looked in to as well. [25,26]

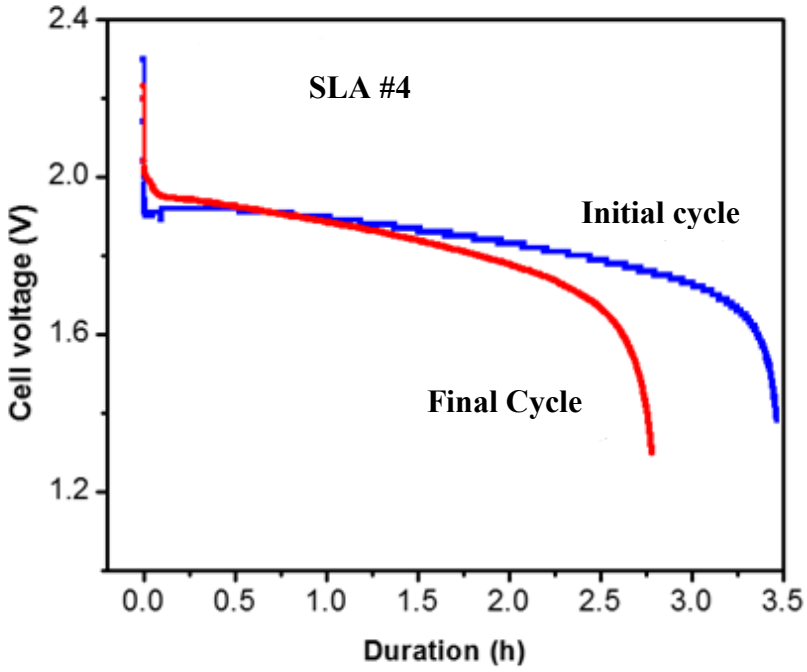

Figure 45: Discharge Profile of Lead Acid Cell #4

Cell #4 represents the condition where the cell is maintained at both high temperature and high charging rate. Initial discharge curves are collected in the same fashion as that for the previous cells. The battery is cycled through nearly hundred cycles with impedance measurement at regular intervals. Once the cycling is over, the final discharge curve is exported and plotted against the initial discharge curve and analyzed. It can be clearly seen that the final discharge curve falls way behind the initial discharge. This automatically leads to the conclusion that this cell exhibits maximum degradation. The reason behind this degradation can be attributed to the effect of high charging rate and high temperature acting together. [27, 28]

From the experimentation and the data analysis conducted above we can infer that Cell #1 is the least degraded cell and Cell #4 is the most degraded cell. Based on this results,

it can be concluded that Charging rate affects degradation and that the additional effect of temperature on it degrades the cell further.[29, 30]

Lithium-ion batteries:

Similar to the sealed lead acid batteries, the lithium ion batteries are also tested at high temperature. But unlike the lead acid batteries, these batteries are maintained at 45 to 50 degrees due to the limitations in the optimum temperature of Lithium ion batteries. All the batteries are discharged at a constant rate (C/3 rate) irrespective of the temperature conditions. Initially a single cell was maintained at room temperature and high charging rate .Since it is a well-known fact that low charging rate at room temperature doesn't have any significant effect, this condition was not tested. Unfortunately, the room temperature Lithium ion cell got bulged twice. Once due to the faultiness of the timer and at the other instance due to overcharging. So, the final discharge curve couldn't be recorded. However the impedance curves and the RHF plots for this cell have been given for the purpose of comparative analysis. [39, 40]

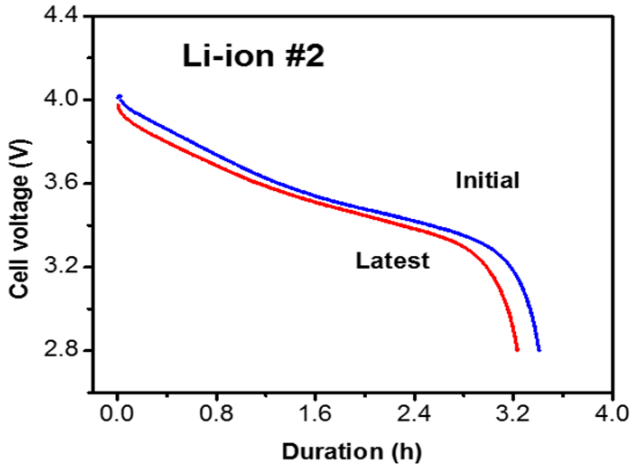

Figure 46 : Discharge Profile of Li-Ion Cell #2

In the above graph, cell #2 is depicted which is maintained at high temperature and low charging rate (C/12 rate). The initial discharge curve is collected in the same manner as for the Lead acid batteries. The battery is cycled for lower number of cycles due to slow rate of charging. The final discharge curve is taken and compared like how it was done before. There is not much degradation found unlike the previous cases. [41, 42]

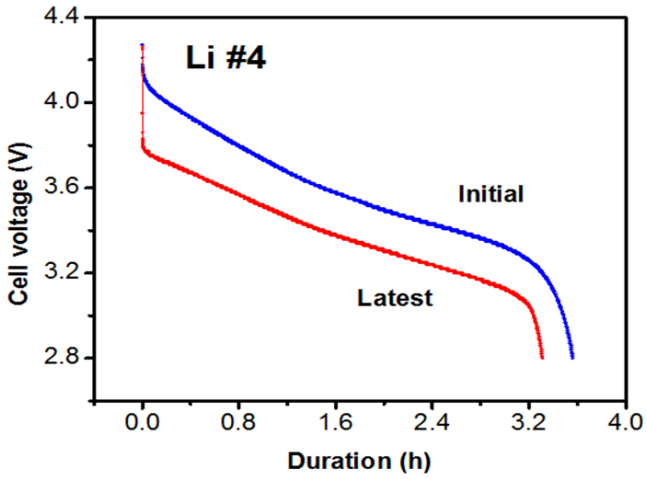

Figure 47: Discharge Profile of Li-Ion Cell #4

The above graph represents Cell #4 which is operated at high temperature and high charging rate. The initial and the final charging curve which is obtained after nearly eighty cycles is exported, plotted in origin and then analyzed. When compared to cell #2, it can be seen that there is a very slight degradation increase in cell #4. Even the Charging rate, which had such a high impact on the Lead acid batteries did not influence the degradation rate in these batteries by a convincing rate. Hence, it can be understood that the lead acid batteries degrade faster than Lithium ion batteries and that if the bulging problem of Li-ion batteries are solved, they would be the best battery technology ever in the market. [43, 44]

4.2 Impedance spectroscopy

Certain parameters like SOC, charge rate, discharge rate, temperature, short-term history or homogeneity of the electrolyte etc. as well as the external contact resistances highly influence the impedance of a lead acid battery. This in turn means that these parameters with the effect of cycling in addition has more influence in the impedance. [31]

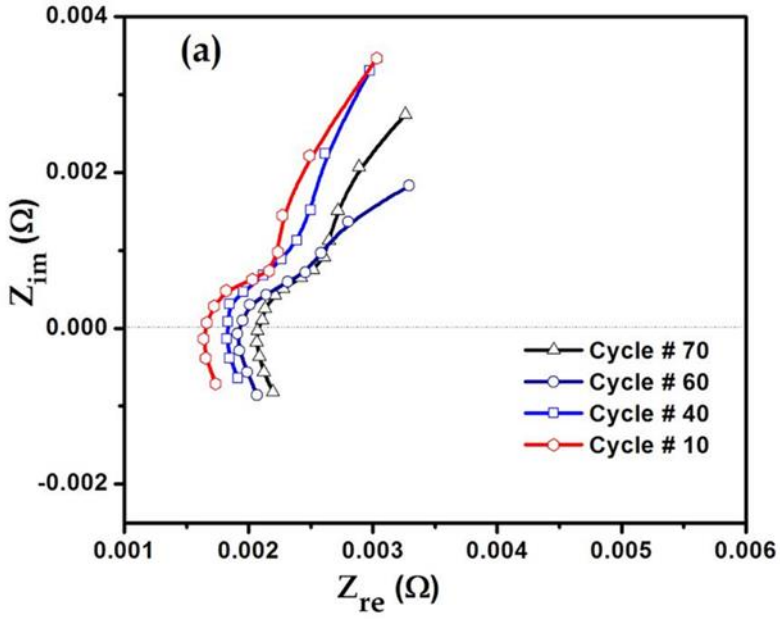

Figure 48: Nyquist plot for Lead Acid Cell #1

The above graph shows the impedance plots exported from the Power Suite software. It represents the Nyquist plots taken during impedance spectroscopy for the cycles 10,40,60,70. The plots tend to increase with the cycle number, but are closely spaced to each other which shows that there is not much increase in impedance .This in turn implies that there is not much degradation. This clearly lies on the same line as the results which were obtained based on the discharge capacity for the same cell. [32]

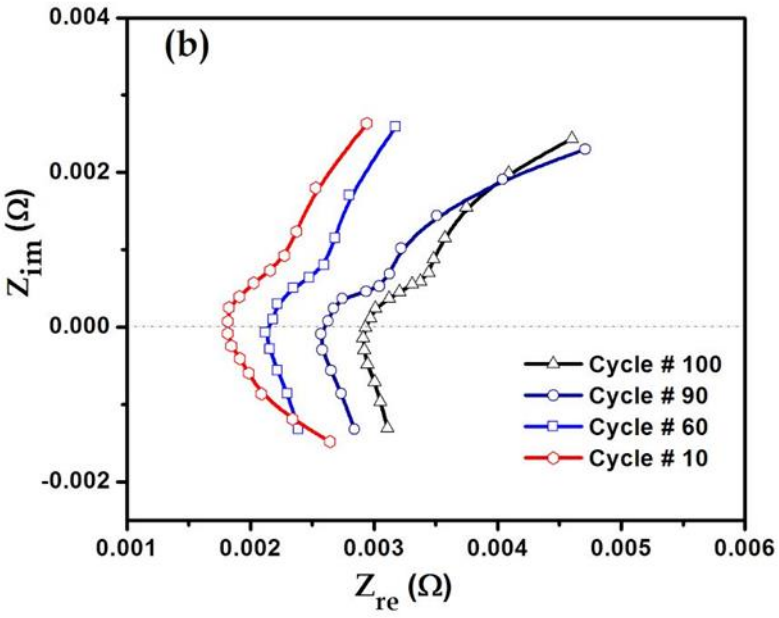

Figure 49: Nyquist plot for Lead Acid Cell #2

The graph above depicts the Nyquist plots obtained from the impedance spectroscopy results for cell #2. Here also there is an increase in the plots along with the cycles. But in this case, there is a considerable increase in the plots as the cycles increase. This clearly indicates that the increase in impedance is very high and so is the degradation. This result is also in correlation with the discharge curves for the same cell. The graph below represents the Nyquist plots obtained for cell # 3. These plots resemble pretty similar to the plots for cell #1 in the sense that they are closely spaced as well. It means that there is no drastic increase in the impedance which further indicates that there is no drastic decrease in the battery capacity. This result is also in support of the result obtained from the discharge curve. Thus a common fact that the influence of temperature is not so high on the batteries, can be inferred from both the test results. [33]

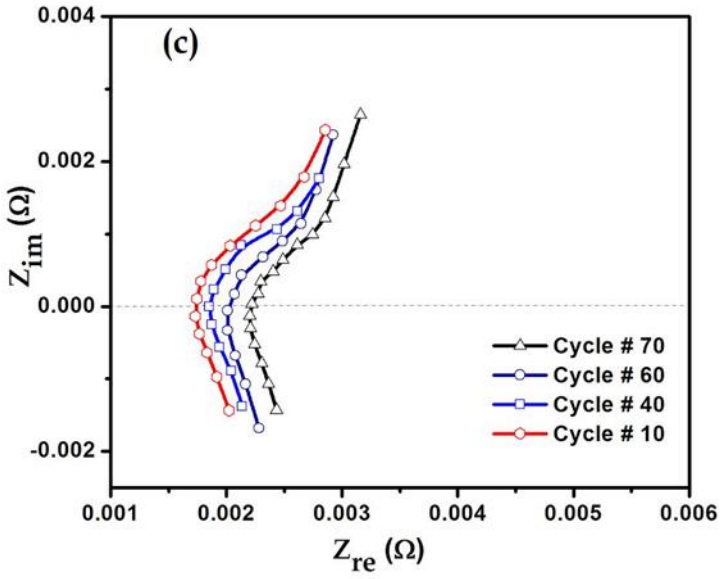

Figure 50: Nyquist plot for Lead Acid Cell #3

Eventually, the Nyquist plots are plotted for cell #4 which represents the High temperature and High Charging rate. These impedance curves are not closely placed as compared to that of Cell #1 and #2.In fact, the curves appear very wide apart from each other. Thus for Cell #4 the increase in impedance is maximum which means that the degradation is maximum for the same cell. Hence it can be concluded that the increase in impedance is maximum for Cell #4 which is due to the combined effect of temperature and charging rate on it. Increase in the impedance can be attributed to several factors that occur within a cell. Two such critical factors which are commonly discussed as reasons behind such impedance increase are grid corrosion and sulfation. [34]

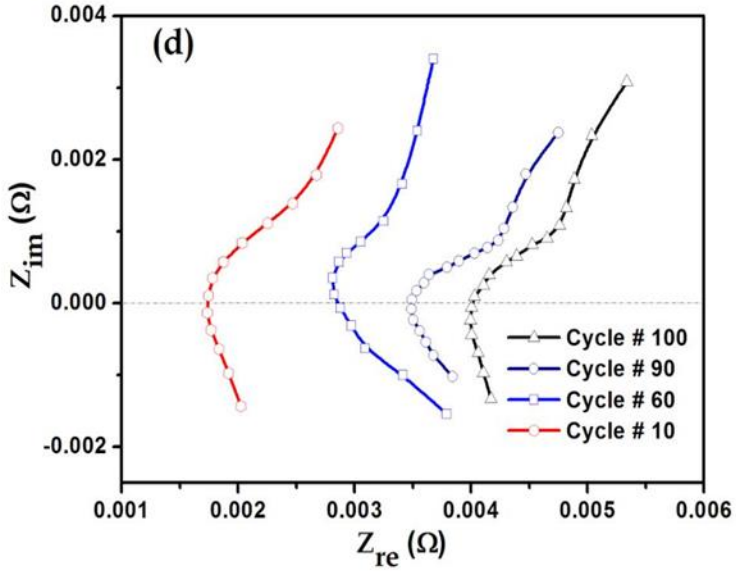

Figure 51: Nyquist plot for Lead Acid Cell #4

There is yet another way to arrive at the the results based on impedance spectroscopy. This is where the High Frequency Resistance (RHF) discussed in the previous section comes into picture. These are nothing but the value of Impedance measured from the Bode phase plot at the zero line. High frequency resistance can also be referred to as the point on the Nyquist plot where zero line from the imaginary axis crosses the nyquist plot. This method can be preferred because of the fact that every cycle observation is reduced to a point which makes more number of observations fit onto the same graph. Nyquist plot looks good only for a set of five to six observations. In most of the cases, the points may not be in such a way that the connecting curve is linear. It would be non-linear in most of the cases. It is not appropriate to show such analysis in non-linear form. So, while representing the RHF data, the points should be fitted and a linear trend line should be added to make the observation look linear. Based on this, the rate at which the cell is decreasing can be found by just calculating the slope. [35, 36]

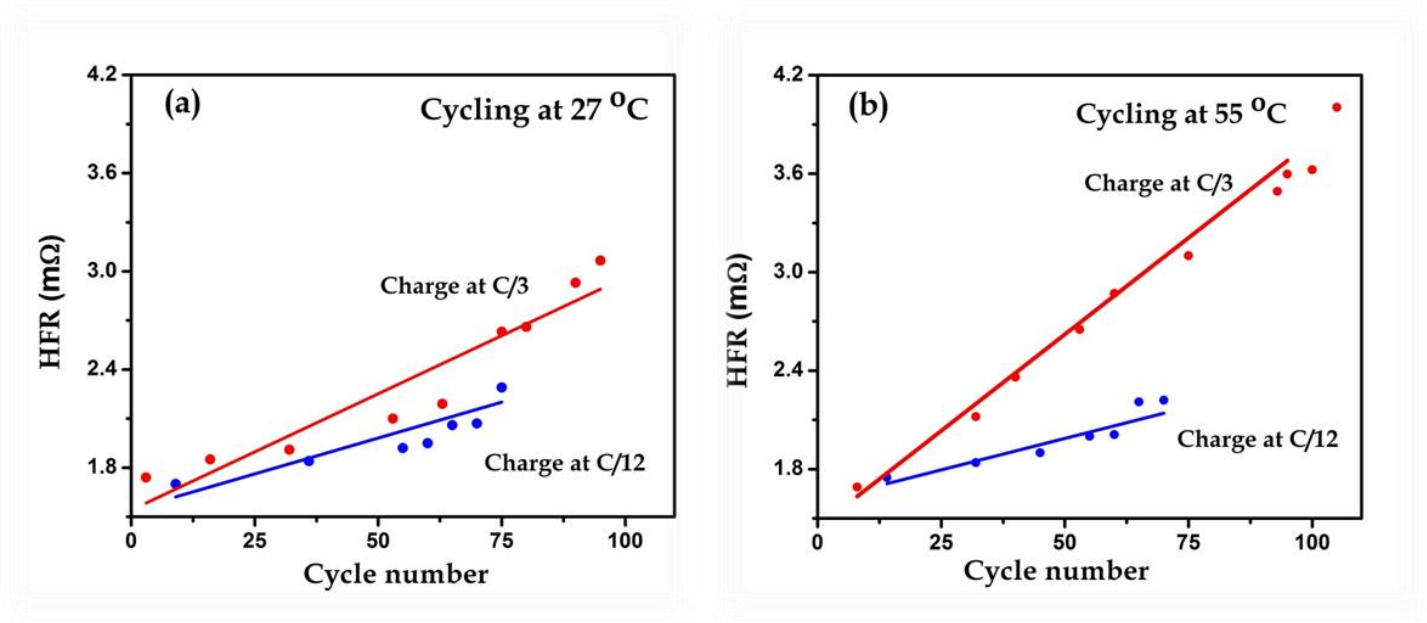

Figure 52: High Frequency Resistance plots for Lead Acid Cells

Rate of increase in HFR is slightly higher when the cell (#2) is charged at faster rate (C/3) compared to that at C/12 rate for cell #1 at room temperature. Similarly, when the cells (#3 and #4) are cycled at High temperature, increase in HFR values is higher for the cell charged at C/3 rate compared to that at C/12 rate. However, the rate of increase in HFR values is extremely high for cell #4 (High Temperature, at C/3 charging rate) compared to that for cell # 2 (Room temperature, at C/3 charging rate) showing the significance of temperature. It is interesting to note that if the charging is done slowly (C/12 rate) then the rate of increase in HFR is not high even at High temperature (cell #3). If we compare the results of the two graphs above they seem to give the same results as the Nyquist plot and the discharge curves. That is the degradation or increase in impedance is high on Cell number #4 due to high temperature and high charging rate whereas it is lowest at the cell where both these conditions are absent. Thus, one can infer that faster rate of charging and

high temperature combination can play a significant role in the degradation of SLA cells. [37, 38]

The curves below represent the Impedance curves of the Lithium ion cells. By examining the three plots it can be seen that there is not much increase in the impedance, except for the third plot. Thus there is not much degradation in the lithium ion cells except for a slightly more degradation in the third plot, which is due to the combined effect of charge rate and high temperature. [45, 46]

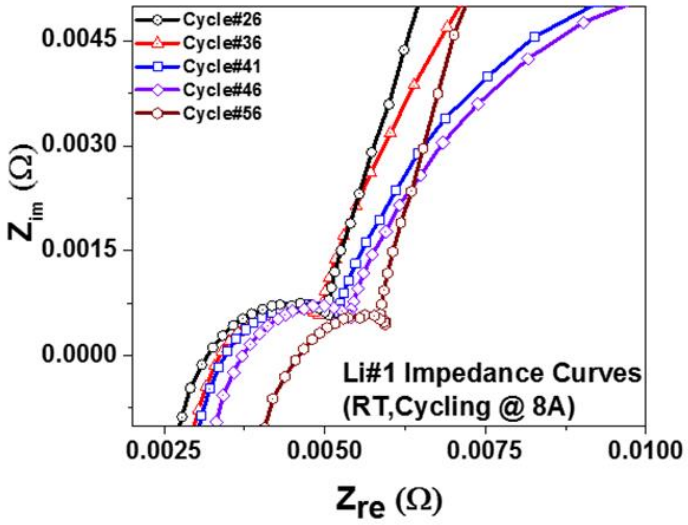

Figure 53: Nyquist plot for Li-Ion Cell #1

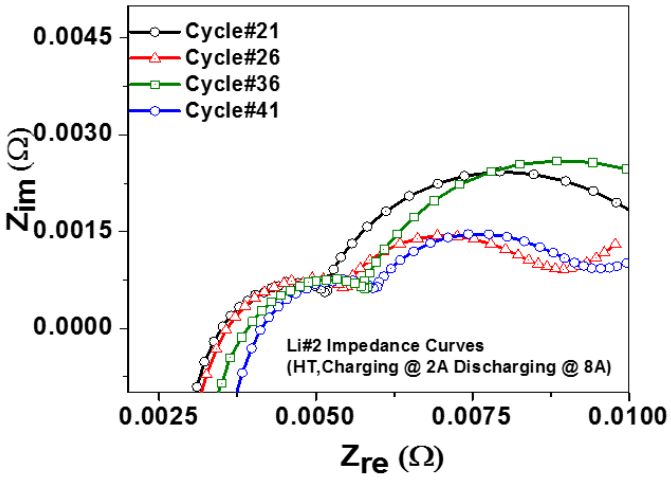

Figure 54: Nyquist plot for Li-Ion Cell #2

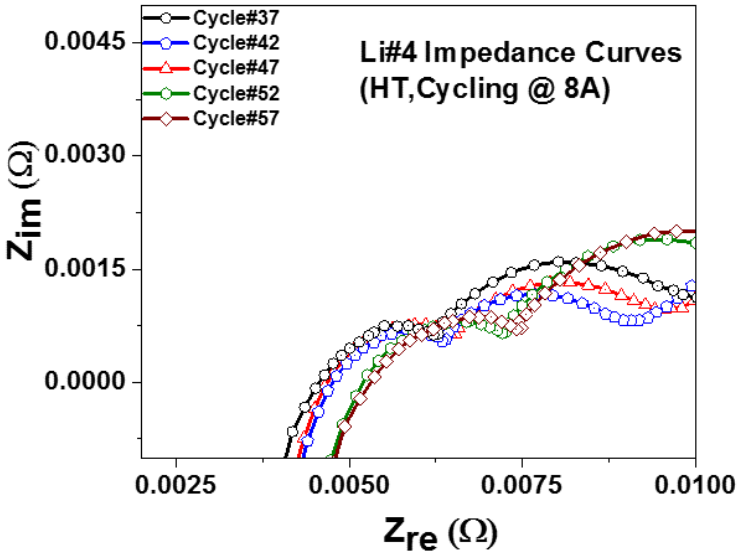

Figure 55: Nyquist plot for Li-Ion Cell #4

The graph below represents the High frequency resistance (RHF) of all the three cells together. These curves are almost linear with not much slope. This indicates that there is not much degradation in the Lithium ion cells when compared to the Sealed Lead Acid cells which are cycled at similar conditions. [47, 48, 49, 50]

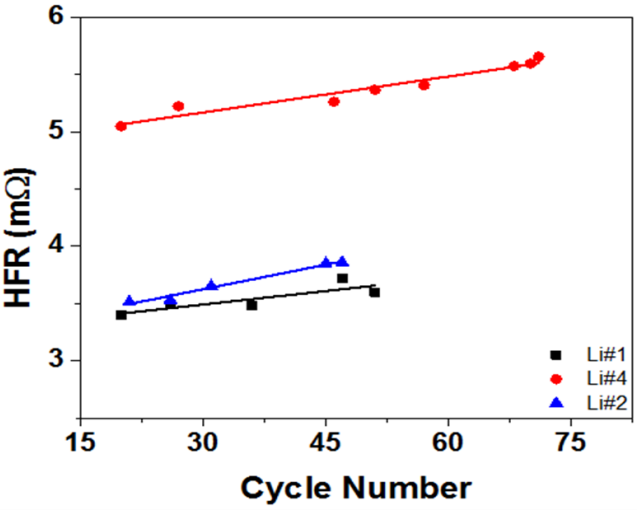

Figure 56: High frequency resistance plot for Li-Ion Cells

4.3 HFR vs SOC

An important and effective method in determining the state of health of the battery is this experiment. The State of Health is plotted against the HFRs measured for individual cells. Initially the cell which is to be tested is fully charged. The time taken to discharge 20 % of the capacity is then found. Initially, when the battery is fully charged, the HFR value is measured and noted against 100 %SOC. The battery is discharged for the time required to discharge to 80%SOC and then HFR value is noted down. In a similar manner, the HFR values are obtained for 60%, 40%, 20%, 0% SOCs and these values are plotted in a graph. This experiment is done for all the four types of lead acid batteries and the plots are made in a single graph.

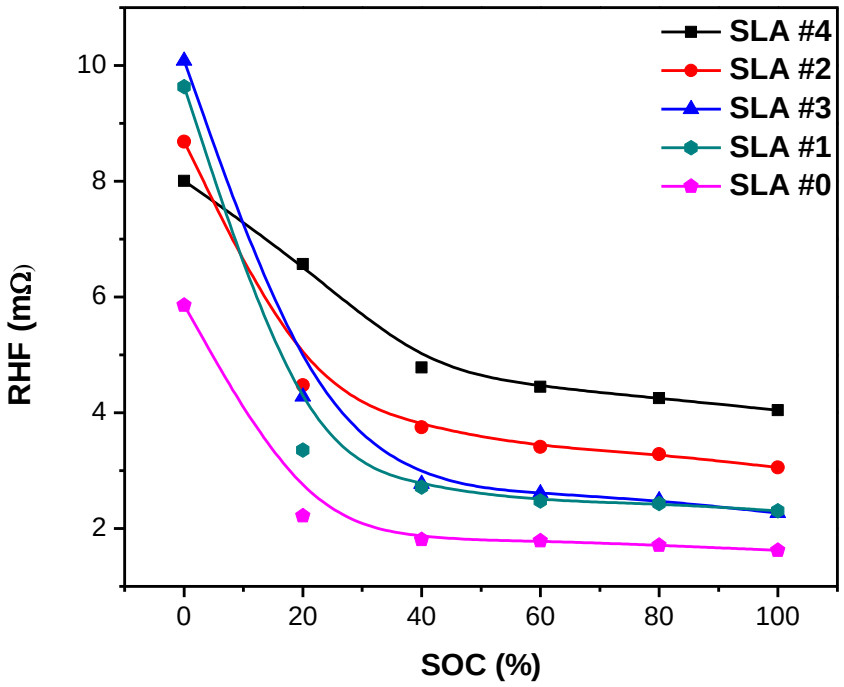

Figure 57: HFR vs SOC test for Lead acid cells

The curve SLA #0 denotes the experiment conducted for a new cell (may be one cycle old). We can infer that as the SOC% increases, there is a decrease in the HFR values for every cell. In order to determine the state of health, the curves should be compared with each other. It can be seen that the newest cell which is hardly cycled is the one having the lowest impedance .It is the bottommost curve in the plot. Above this curve is the curve of Cell #1, indicating that it is the cell with the lowest value of degradation and the lowest HFR values. Cell #3 has its impedance curve slightly above indicating that there is not much degradation and change in impedance compared to Cell #1. Cell #2 which is cycled at room temperature but high C rate comes immediately above. Finally comes Cell #4 which is maintained at high temperature and high charging rate, comes as the topmost curve. This clearly indicates the fact that, based on the placement of a curve in the plot, its state of heath can be measured

relative to the state of health of the other batteries. This experiment also arrives at a common conclusion that the state oh health of a battery is influenced a lot by the interaction of high temperature and high charge rate. If these two parameters are compared to each other, Charge rate has the clear edge over temperature in influencing the state of health of a battery. This method of State of health determination is one of the most effective and highly accurate methods. Performing this experiment is not very easy since the personnel should be present all the time when the test is going on. It might take nearly four to four and half hours to complete the experiment for a single cell. Thus, only two to three cells can be tested in a single day depending upon the user person carrying out the process. While conducting this experiment it should be made sure that normal cycling of the battery should not be conducted in-between once this process has been started. This experiment also delivers the same results as that of the discharge curve and impedance spectroscopy measurements. The table below denotes the readings which are taken during the experiment. [34, 36, 37]

Table 2 : HFR vs SOC data for Lead Acid cells

SOC %	RHF (mΩ)				
	#4	#2	#3	#1	#0
100	4.046	3.054	2.27	2.305	1.621
80	4.252	3.286	2.488	2.434	1.712
60	4.448	3.408	2.605	2.478	1.787
40	4.781	3.748	2.769	2.715	1.807
20	6.566	4.477	4.28	3.353	2.22
0	8.007	8.682	10.08	9.634	5.857

CHAPTER FIVE

5. CONCLUSION

The results obtained from various experiments gave a complete perspective on the state of health determination of a battery at different climatic conditions. It provided a convenient and effective means by which selection of batteries based on the weather conditions can be done. Also, it can be used to guide the manufacturers of battery chargers in designing the appropriate charger. The sole purpose of the result is to arrive at a single parameter which would determine the State of health .Based on the results obtained, it can be made clear that Impedance is the single deciding factor that determines the state of health of the battery. Impedance is taken as an important entity due to the fact that the Impedance is the combination of both resistance and capacitance included in the battery. Hence it is wise to measure the impedance rather than measuring the battery resistance. The results from this research are also focused to assist a parallel project which involves the designing of the impedance measuring device Bat-Z- tester. This device would give the impedance of the battery directly when connected to its leads. Based on this impedance or RHF value, comparison is made between the corresponding values obtained as High frequency resistance from the experiments. In simple words, these experimental results can be used as a logarithmic table .This would easily help in determining the State of health of a battery in one shot, whose history is totally unknown. Irrespective of the battery technology used, a common conclusion that the charging rate has more influence in the state of health than the temperature. When comparison is made between the lead acid and Lithium-ion cells it can be concluded that the degradation of the state of health is more in the former than in the latter. However Lead acid batteries still find some applications in the market because

of the ease of handling, maintenance and cost effectiveness. When it comes to lithium-ion cells, the degradation is minimum and there is very less effect of charging rate on the state of health. In spite of this major advantage, a major issue which limits the usage of this technology is bulging. If this issue is addressed, this technology would undoubtedly be the best ever battery in the market.

REFERENCES

1. Bergstrom, Sven. Nickel–Cadmium Batteries – Pocket Type. Journal of the Electrochemical Society, The Electrochemical Society, September 1952.

2. Ellis, G. B., Mandel, H., and Linden, D. Sintered Plate Nickel–Cadmium Batteries. Journal of the Electrochemical Society, The Electrochemical Society, September 1952.

3. A.M. Kannan, (2014). State of health determination of sealed lead acid battery under various operating conditions. ***Journal of Power Sources***. 261 (Submitted on 4 April 2014).

4. Panasonic USA (2010). Rechargeable Li-Ion OEM Battery Products. [ONLINE] Available at: http://www.panasonic.com/industrial/batteries-oem/oem/lithium-ion.aspx. [Last Accessed 23 April 2010].

5. ThermoAnalytics, Inc. (2007). HEV Vehicle Battery Types. [ONLINE] Available at: http://www.thermoanalytics.com/support/publications/batterytypesdoc.html. [Last Accessed 11 June 2010].

6. epanorama (2009). Battery Power Supply Page. [ONLINE] Available at: http://www.epanorama.net/links/psu_battery.html. [Last Accessed 10 July 2009].

7. West Mountain Radio (2014). Computerized Battery Analyzer. [ONLINE] Available at: http://www.westmountainradio.com/cba.php.

8. CircuitSpecialists (2014). 300 Watt 360 Volt Programmable DC Electronic Load. [ONLINE] Available at: http://www.circuitspecialists.com/dc-electronic-load-csi3711a.html .

9. Jasco Products (1999). GE 24-Hour Two-Outlet Mechanical Timer User Manual. [ONLINE] Available at: http://www.jascoproducts.com/support/manual-downloads/applications/DocumentLibraryManager/upload/Plug-In-15075-Manual-eng.pdf. [Last Accessed 2014].

10. Hydrofarm (2014). 7 Day Dual Outlet Digital Timer. [ONLINE] Available at: http://www.hydrofarm.com/product.php?itemid=4168. [Last Accessed 2014].

11. J. Vetter, (2006). In situ study on CO2 evolution at lithium-ion battery cathodes. Journal of Power Sources. 159 (1), pp.277-281.

12. M. Holzapfel, (2007). Oxygen, hydrogen, ethylene and CO2 development in lithium-ion batteries. Journal of Power Sources. 174 (2), pp.1156–1160.

13. M. Wu, (2004). Correlation between electrochemical characteristics and thermal stability of advanced lithium-ion batteries in abuse tests—short-circuit tests. Electrochimica Acta. 49 (11), pp.1803–1812.

14. C. Yuan, (2014). Mathematical modeling of the electrochemical impedance spectroscopy in lithium ion battery cycling. Electrochimica Acta. 127, pp.266–275.

15. T.G Chang, (2000). Structural changes of active materials and failure mode of a valve-regulated lead-acid battery in rapid-charge and conventional-charge cycling. Journal of Power Sources. 91 (2), pp.177–192.

16. G. Papazov, (1996). Influence of cycling current and power profiles on the cycle life of lead/acid batteries. Journal of Power Sources. 62 (2), pp.193–199.

17. C. Brissaud, (1997). Structural and morphological study of damage in lead/acid batteries during cycling and floating tests. Journal of Power Sources. 64 (1-2), pp.117–122.

18. D.C. Montgomery, (1982). Introduction to Linear Regression Analysis. 3rd ed. USA and Canada: John Wiley & Sons, Inc.

19. A. Eddahech, (2012). Behavior and state-of-health monitoring of Li-ion batteries using impedance spectroscopy and recurrent neural networks. Electrical Power and Energy Systems. 42, pp.487-494.

20. D.U. Sauer, (2005). Impedance measurements on lead–acid batteries for state-of-charge, state-of-health and cranking capability prognosis in electric Abstract and hybrid electric vehicles. Journal of Power Sources. 144, pp.418–425.

21. S. Schaeck, (2011). Lead-acid batteries in micro-hybrid applications. Part II. Test proposal. Journal of Power Sources. 196 (3), pp.1555–1560.

22. R. Inguanta, (2014). High-performance of PbO2 nanowire electrodes for lead-acid battery. Journal of Power Sources. 256, pp.72-79.

23. K. Maeda, (2013). Novel charge/discharge method for lead acid battery by high-pressure crystallization. Journal of Crystal Growth. 373, pp.138-141.

24. B.Y. Liaw, (2011). Effect of discharge rate on charging a lead-acid battery simulated by mathematical model. Journal of Power Sources. 196 (7), pp. 3414-3419.

25. S. Farhad, (2013). Effect of convective mass transfer on lead-acid battery performance. Electrochimica Acta. 97, pp.278-288.

26. S. Park, (2014). An analytical study of a lead-acid flow battery as an energy storage system. Journal of Power Sources. 249, pp.207-218.

27. S. Piller, (2001). Methods for state-of-charge determination and their applications. Journal of Power Sources. 96 (1), pp.113-120.

28. N. Munichandraiah, (2000). A review of state-of-charge indication of batteries by means of a.c. impedance measurements. Journal of Power Sources. 87 (1-2), pp.12-20.

29. S.K. Martha, (2005). Assembly and performance of hybrid-VRLA cells and batteries. Journal of Power Sources. 144 (2), pp.560-567.

30. R. López, (2014). Comparison of different lead–acid battery lifetime prediction models for use in simulation of stand-alone photovoltaic systems. Applied Energy. 115, pp.242-253.

31. K. Chao, (2011). State-of-health estimator based-on extension theory with a learning mechanism for lead-acid batteries. Expert Systems with Applications. 38 (12), pp.15183–15193.

32. F. Huet, (1998). A review of impedance measurements for determination of the state-of-charge or state-of-health of secondary batteries. Journal of Power Sources. 70 (1), pp.59-69.

33. Y. Çadırcı, (2004). Microcontroller-based on-line state-of-charge estimator for sealed lead–acid batteries. Journal of Power Sources. 129 (2), pp.330–342.

34. N. Khare, (2012). A novel magnetic field probing technique for determining state of health of sealed lead-acid batteries. Journal of Power Sources. 218, pp.462–473.

35. H. Meiwes, (2011). Influence of measurement procedure on quality of impedance spectra on lead–acid batteries. Journal of Power Sources. 196 (23), pp.10415–10423.

36. Glen Alber. Predicting Battery Performance using internal cell resistance. [ONLINE] Available at: http://www.alber.com/Docs/PredictBatt.pdf .

37. S. Choe, (2010). One-dimensional dynamic modeling and validation of maintenance-free lead-acid batteries emphasizing temperature effects. Journal of Power Sources. 195 (20), pp.7102–7114.

38. T Hatanaka, (1998). Small-capacity valve-regulated lead/acid battery with long life at high ambient temperature. Journal of Power Sources. 73 (1), pp.98–103.

39. C. C. Mi, (2013). A new method to estimate the state of charge of lithium-ion batteries based on the battery impedance model. Journal of Power Sources. 233, pp.277–284.

40. B. Wang, (2014). An electrochemistry-based impedance model for lithium-ion batteries. Journal of Power Sources. 258, pp.9-18.

41. W. Waag, (2013). Experimental investigation of the lithium-ion battery impedance characteristic at various conditions and aging states and its influence on the application. Applied Energy. 102, pp.885-897.

42. U. Tröltzsch, (2006). Characterizing aging effects of lithium ion batteries by impedance spectroscopy. Electrochimica Acta. 51 (8-9), pp.1664–1672.

43. T Osaka, (2003). Influence of capacity fading on commercial lithium-ion battery impedance. Journal of Power Sources. 119–121, pp.929–933.

44. M. Ecker, (2012). Development of a lifetime prediction model for lithium-ion batteries based on extended accelerated aging test data. Journal of Power Sources. 215, pp.248–257.

45. Y. Xing, (2014). State of charge estimation of lithium-ion batteries using the open-circuit voltage at various ambient temperatures. Applied Energy. 113, pp.106-115.

46. K. Amine, (2001). Factors responsible for impedance rise in high power lithium ion batteries. Journal of Power Sources. 97-98, pp.684-687.

47. C.W. Hong, (2013). Integrated modeling for the cyclic behavior of high power Li-ion batteries under extended operating conditions. Applied Energy. 111, pp.681–689.

48. J. Vetter, (2005). Ageing mechanisms in lithium-ion batteries. Journal of Power Sources. 147 (1-2), pp. 269–281.

49. B.N Popov, (2000). Studies on capacity fade of lithium-ion batteries. Journal of Power Sources. 91 (2), pp.122-129.

50. F. Fischer, (2013). Lithium secondary batteries working at very high temperature: Capacity fade and understanding of aging mechanisms. Journal of Power Sources. 236, pp.265.